SEMMELWEIS EGYETEM

DOKTORI ISKOLA

Ph.D. értekezések

3359.

FJOLLA ZHUBI BAKIJA

Szív-és érrendszeri betegségek élettana és klinikuma

című program

Programvezető: Dr. Merkely Béla, egyetemi tanár

Témavezetők: Dr. Kovács Attila, egyetemi adjunktus

Dr. Fábián Alexandra, szakorvosjelölt

PROGNOSTIC ROLE OF ADVANCED ECHOCARDIOGRAPHY IN CARDIOVASCULAR RISK ASSESSMENT: INSIGHTS FROM A COMMUNITY-BASED SCREENING PROGRAM

Ph.D. thesis

Fjolla Zhubi Bakija MD

Doctoral College, Cardiovascular Medicine and Research Division
Semmelweis University

Supervisors: Attila Kovács MD, DSc
Alexandra Fábián MD, PhD

Official reviewers: Ágnes Nógrádi MD, PhD
Györgyi Csósza MD, PhD

Head of the Complex Examination Committee: Prof. Zoltán Ungvári MD, PhD

Members of the Complex Examination Committee: Sándor Nardai MD, PhD
Gergely Ágoston MD, PhD

Budapest
2026

Table of Contents

List of abbreviations

2D – two-dimensional

A – atrial contraction

a' – peak late (atrial) diastolic annular velocity

ACC/AHA- American College of Cardiology/American Heart Association

ASCVD - atherosclerotic cardiovascular disease

AUC – area under the curve

BMI – body mass index

BSA – body surface area

CABG – coronary artery bypass grafting

CI – confidence interval

CT – computed tomography

CVD – cardiovascular disease

DT – deceleration time

E – early diastolic filling

e' – early diastolic annular velocity

ECG – electrocardiography

EDV – end-diastolic volume

EDVi – end-diastolic volume index

EF – ejection fraction

eGFR – estimated glomerular filtration rate

ESV – end-systolic volume

ESVi – end-systolic volume index

ET – ejection time

FT – filling time

GCW – global constructive myocardial work

GLS – global longitudinal strain

GWE – global myocardial work efficiency

GWI – global myocardial work index

GWW – global myocardial wasted work

HbA1C – glycated hemoglobin

HDL – high-density lipoprotein

HFpEF – heart failure with preserved ejection fraction

HR – hazard ratio

IMT – intima-media thickness

IVCT – isovolumetric contraction time

IVRT – isovolumetric relaxation time

IVSd – interventricular septum dimension

LA – left atrium

LAVi – left atrial volume index

LDL – low-density lipoprotein

LV – left ventricle

LVIDd – left ventricular internal diameter at end-diastole

LVMi – left ventricular mass index

MI – myocardial infarction

MW – myocardial work

PACS – peak atrial contraction strain

PALS – peak atrial longitudinal strain

PCI – percutaneous coronary intervention

ProBNP – pro-B-type natriuretic peptide

PWd – posterior wall dimension

RA – right atrium

RAVi – right atrial volume index

ROC – receiver operating characteristic

ROI – region of interest

RV – right ventricle

RVd – right ventricular dimension

RWT – relative wall thickness

s’ – systolic annular velocity

SCORE 2 – Systematic Coronary Risk Evaluation 2

SCORE 2–OP – Systematic Coronary Risk Evaluation 2 - Older Persons

SD – standard deviation

STE – speckle-tracking echocardiography

TAPSE – tricuspid annular plane systolic excursion

TDI – tissue Doppler imaging

WHO – World Health Organization

1. Introduction

1.1. Preventive cardiology: The importance of cardiovascular risk assessment

Preventive cardiology represents a fundamental domain within cardiovascular medicine dedicated to identifying and mitigating risk factors to prevent the onset of cardiac diseases, reduce the incidence of first-time cardiovascular events, and slow disease progression in individuals with established cardiovascular conditions (1). The importance of preventive cardiology has grown significantly in recent decades, in parallel with the rising global burden of cardiovascular diseases (CVD) and in light of increasing cardiovascular morbidity and mortality rates (1, 2). Even to this day, cardiovascular diseases remain the leading cause of mortality worldwide, accounting for approximately 17.9 million deaths in 2019, equivalent to 32% of all global deaths (2). In response, the World Health Organization (WHO) has prioritized CVD within its global action plan, aiming to reduce cardiovascular mortality by 25% by the year 2025, a goal that necessitates more precise and effective strategies for risk prediction and prevention (3).

A main focus of preventive cardiology is to reduce the global burden of CVD by targeting well-established modifiable risk factors such as hypertension, dyslipidaemia, diabetes, smoking, and obesity. Previous large-scale epidemiological research has demonstrated that more than 90% of myocardial infarctions worldwide can be attributed to modifiable risk factors, underscoring the critical importance of primary prevention efforts on public health outcomes. Moreover, effective management of these risk factors through lifestyle intervention and evidence-based pharmacotherapy has been shown to significantly reduce the incidence of major cardiovascular events (4). Nevertheless, despite significant advances in therapeutic options, research still shows that inadequate control of risk factors remains a major contributor to the persistently high global prevalence of CVD (5). Furthermore, studies indicate that adherence to preventive strategies not only improves survival and quality of life but also contributes to lower rates of hospitalization and reduced healthcare expenditures (6). Therefore, the systematic integration of structured preventive cardiology programmes into

clinical practice is essential to address the continued global threat posed by CVD and to ensure a sustainable, population-level impact on long-term cardiovascular health (7, 8).
Given the compelling evidence supporting primary and secondary prevention, integrating structured preventive cardiology programmes into routine healthcare practice is essential for mitigating the growing impact of CVD on public health. However, to translate preventive strategies into measurable clinical benefits, accurate cardiovascular risk assessment tools are essential. Risk stratification serves as a crucial link between population-level recommendations and individualized patient care. Consequently, the success of preventive cardiology relies not only on effective therapeutic options but also on accurate risk evaluation, underscoring the need for evidence-based methods of cardiovascular risk estimation to guide early and personalized preventive measures.

1.1.1 Estimation of cardiovascular risk: use of traditional risk prediction models

Accurate cardiovascular risk assessment is a fundamental component of preventive cardiology, enabling early identification and targeted intervention for individuals at increased risk of CVD. Over the years, several risk prediction models have been developed to estimate the likelihood of future cardiovascular events, with the most widely adopted being the SCORE2 (Systematic Coronary Risk Evaluation 2), the updated SCORE2-OP (SCORE2-Older Persons) the American College of Cardiology/American Heart Association (ACC/AHA) pooled cohort equations, and the Framingham Risk Score (9-12).
SCORE2, an updated version of the original SCORE model, provides risk estimation based on large-scale European cohort data. It incorporates core variables such as age, sex, smoking status, blood pressure, and cholesterol levels to predict both fatal and non-fatal cardiovascular events over a 10-year period, with improved applicability across different European regions with varying baseline risk profiles (7, 9, 13). The ACC/AHA pooled cohort equations, predominantly utilized in the United States, serve a similar function by estimating the 10-year risk of atherosclerotic cardiovascular disease (ASCVD), including both coronary heart disease and stroke, and as such, providing particularly valuable information for guiding therapeutic recommendations (10, 14). The Framingham Risk Score, originally derived from the landmark Framingham Heart Study, played a pioneering role in systematic cardiovascular

risk prediction by focusing primarily on coronary heart disease outcomes. However, its generalizability is often limited due to population-specific variations, leading to decreased accuracy in ethnically and demographically diverse groups and contemporary cohorts (11). Although these traditional models remain the cornerstone of cardiovascular risk estimation, their accuracy may become limited in certain populations with more complex clinical characteristics. For instance, in elderly individuals, risk assessment is complicated by age-related physiological changes and the cumulative burden of comorbidities, factors that are not fully captured by conventional scoring systems. Similarly, obesity introduces a range of metabolic and hemodynamic alterations that influence cardiovascular risk but are often insufficiently reflected in traditional models. Importantly, neither aging nor obesity constitutes cardiovascular disease per se, and many individuals within these groups remain free of overt pathology. Nonetheless, accurate risk stratification remains a challenge. These considerations underscore the need for complementary approaches that can reveal subclinical alterations in cardiac structure and function, thereby refining risk prediction in these nuanced populations.

1.1.1.1 Challenges of risk stratification of the elderly

Cardiovascular risk assessment in older adults presents unique challenges due to age-related physiological changes, the burden of multimorbidity, and the inherent limitations of conventional risk models. Commonly implemented predictive tools, such as SCORE2, the Framingham Risk Score, and the ACC/AHA Pooled Cohort Equations, all demonstrated limited accuracy in elderly populations (9-11). Recently, to further update the accuracy of risk predictions, SCORE2-OP, a competing risk-adjusted model for individuals aged over 70 years without pre-existing CVD, was developed and validated, as a recalibrated version of the SCORE2 model to estimate 5- and 10-year risk of incident CVD (12). Still, these models may either underestimate or overestimate risk due to age-associated alterations in cardiovascular physiology, including increased vascular stiffness, left ventricular hypertrophy, and diastolic dysfunction, which are not fully captured by traditional scoring systems (15, 16). Additionally, the generally elevated baseline cardiovascular risk in older individuals diminishes the discriminatory power of these models, limiting their ability to stratify individuals into meaningful risk categories.

In the elderly, traditional risk factors such as cholesterol levels and blood pressure exhibit attenuated predictive value compared to younger populations, partially due to complex interactions between physiological aging and coexisting comorbidities (17, 18).

Another significant limitation is the frequent presence of subclinical CVD in older adults, which often remains undetected using conventional risk markers alone. Many elderly individuals exhibit silent atherosclerosis, myocardial fibrosis, diastolic dysfunction, or early-stage heart failure with preserved ejection fraction (HFpEF) that is often unrecognized by traditional risk prediction models (15, 16, 19). Therefore, refining cardiovascular risk assessment in the elderly may require a shift from traditional scoring systems toward a more integrative approach that accounts for age-related physiological changes, subclinical cardiac alterations, and competing health risks.

1.1.1.2 Challenges in cardiovascular risk estimation: the impact of obesity

The prevalence of overweight and obesity is rising globally, affecting populations across both developed and developing regions. According to the WHO, approximately 2.5 billion adults worldwide, around 43% of the global population, are classified as overweight, with a staggering 890 million individuals estimated to be living with obesity (20). In European countries affiliated with the European Society of Cardiology, approximately one in five adults meets the criteria for obesity (21). Given its well-established impacts on morbidity, mortality, and healthcare systems, obesity still represents a critical and growing health concern worldwide.

Overweight and obesity are characterized by abnormal or excessive fat accumulation that poses significant health risks (20). Research has long established a link between obesity and increased mortality, as well as heightened risk for cardiovascular morbidity and mortality (22-24). While earlier studies primarily attributed the connection between increased adiposity and cardiovascular mortality to indirect mechanisms, such as the exacerbation of risk factors and chronic conditions, recent findings indicate that direct mechanisms also contribute to this relationship (25, 26). Recent studies have shown that individuals previously classified as "metabolically healthy obese" are at a higher risk of coronary heart disease, cerebrovascular disease, and heart failure compared to their metabolically healthy normal-weight counterparts (25, 27). Overall, the interplay of increased cardiac workload and metabolic dysregulation renders individuals with obesity particularly susceptible to progressive cardiovascular pathology, even in the absence of conventional risk factors.

In this context, non-invasive and widely available imaging modalities—particularly echocardiography—have gained prominence for their ability to detect early functional cardiac changes associated with excess adiposity, offering a practical and feasible approach to refine cardiovascular risk assessment in this heterogeneous population.

Given the nuanced and often silent progression of cardiovascular deterioration in both elderly and obese individuals, conventional risk models alone may be insufficient for accurate risk stratification. These populations frequently exhibit early functional changes that remain undetected by standard clinical assessments. This gap highlights the need for added screening tools that can detect early cardiac involvement before overt disease develops. Echocardiography, with its ability to non-invasively assess both structural and functional cardiac parameters, offers a valuable opportunity to enhance risk assessment where traditional models reach their limitations.

1.2 Advanced Echocardiographic Techniques in Cardiovascular Risk Assessment

Despite the widespread utility of traditional cardiovascular risk prediction models, their capacity to accurately stratify risk in individuals without overt disease remains limited, particularly among subgroups such as the elderly and those with obesity, where physiological and metabolic complexity often obscures early pathological processes (15-18, 23, 25). Both age-related cardiovascular remodelling and the diverse cardiometabolic effects of adiposity may precede clinical manifestations yet remain undetected by standard scoring systems. As such, there is a growing need to integrate additional tools capable of identifying preclinical alterations in cardiac structure and function. Therefore, non-invasive imaging modalities—most notably echocardiography—have emerged as valuable tools for aiding clinical risk assessment, offering the potential to enhance prognostic accuracy through the early detection of subclinical myocardial dysfunction (28-30).

Besides other advanced imaging techniques such as coronary artery calcium scoring, carotid intima-media thickness (IMT) quantification, echocardiography has become a cornerstone screening and diagnostic tool for cardiovascular risk assessment, during the past decades, particularly valuable in low-risk populations due to its non-invasive nature, cost-effectiveness, and accessibility (31-33).

As part of most routine clinical echocardiographic protocols, left ventricular (LV) ejection fraction (EF) is a prime measure of systolic function, despite its several well-recognized limitations (34). It is highly load-dependent, influenced by changes in preload and afterload, and reflects volumetric changes rather than myocardial deformation, making it less sensitive to detect early myocardial dysfunction. Additionally, it relies on geometric assumptions, particularly in 2D imaging (35, 36). Consequently, acknowledging these shortcomings has led to increased interest in more sensitive and reproducible modalities such as speckle-tracking echocardiography (STE) and myocardial work (MW) analysis. Speckle-tracking echocardiography offers a solution to detect more subtle functional changes as it allows for the identification of subclinical LV systolic dysfunction in not only patients with distinct CVDs but also in specific low-risk subgroups, such as individuals with obesity, indicating early cardiac impairment despite preserved LVEF (35, 36). As an early indicator of cardiac dysfunction, STE-derived global longitudinal strain (GLS) may be useful in identifying those who are at a greater risk of cardiovascular morbidity and mortality. Indeed, recent studies reported that GLS could bear added value in predicting cardiovascular adverse outcomes in the general population (31, 32). Furthermore, most recently, novel echocardiographic techniques, such as non-invasive LV pressure-strain loop-derived MW analysis have gained increased attention as they provide more in-depth insight into LV contractility that extends beyond more traditional measures like LVEF and GLS (37, 38) as it accounts for afterload, allowing a more accurate assessment of systolic function (38).

Beyond systolic function, assessment of diastolic function is of great importance, as LV diastolic dysfunction has similar detrimental downstream consequences in the long term (39-41). Besides conventional approaches, the assessment of LV diastolic function along with left atrial (LA) function may offer more sensitive biomarkers to detect early dysfunction and predict long-term prognosis (30, 40, 42). Since diastolic impairment frequently precedes systolic dysfunction in aging populations, its detection could aid timely and refined cardiovascular risk assessment in the elderly (30). Advanced echocardiographic techniques, such as STE, could offer a clinically feasible and cost-effective approach to improving cardiovascular risk prediction in the aging population.

1.2.1 Speckle-tracking echocardiography

1.2.1.1 Left Ventricular Global Longitudinal Strain

Speckle-tracking echocardiography emerged as an advanced imaging modality enabling the quantitative assessment of myocardial deformation (34) by tracking the natural acoustic markers, known as "speckles", within standard 2D grayscale images. These speckles, generated by the reflection, refraction, and scattering of ultrasound beams, serve as stable reference points that the software follows frame-by-frame throughout the cardiac cycle within a predefined region of interest (ROI) (43, 44). This technique allows for objective and reproducible evaluation of myocardial strain, expressed as a percentage change in myocardial length relative to its baseline dimension. Shortening of myocardial fibres is conventionally represented by negative strain values, while lengthening is depicted as positive (44, 45).

Myocardial deformation can be assessed in multiple dimensions, including longitudinal, circumferential, and radial directions. Among these, longitudinal strain, reflecting the contraction of subendocardial fibres oriented along the long axis of the LV, has gained particular clinical relevance (44, 45). These subendocardial fibres are particularly susceptible to ischemia, hemodynamic overload, and stress due to their elevated metabolic demand. Consequently, compared to other functional parameters, longitudinal strain often exhibits earlier impairment in various cardiovascular diseases, serving as a particularly sensitive marker for early myocardial dysfunction (44, 45).

Global longitudinal strain, a widely used metric that quantifies the average longitudinal deformation across all left ventricular segments, has demonstrated superior clinical utility over traditional functional indices such as LVEF. GLS provides incremental prognostic value across a wide range of cardiovascular diseases (44, 46-49). Studies have shown that GLS is particularly useful in detecting subclinical myocardial dysfunction, identifying early changes in cardiotoxicity, and predicting adverse outcomes in conditions such as heart failure, ischemic heart disease, valvular heart disease, and cardiomyopathies. Furthermore, GLS serves as an early marker of cardiac dysfunction and can help identify individuals at higher cardiovascular risk even within the general population (31, 32).

1.2.1.2 Peak atrial longitudinal strain

Speckle-tracking echocardiography extends beyond ventricular analysis and can be applied to the left atrium (LA) to assess its mechanical function, offering valuable insights into diastolic function. In the context of LA strain analysis, the ROI is defined by tracing the endocardial border using both four- and two-chamber views for biplane calculations to avoid foreshortening (50). However, recent research, including a meta-analysis, supports the clinical acceptability of single apical views for LA strain assessment (51).

Left atrial deformation occurs in three distinct phases - reservoir, conduit, and contraction - each corresponding to a particular phase of the cardiac cycle with unique functional roles (51). During the reservoir phase, which begins at the end of ventricular diastole and continues until mitral valve opening, the LA expands as it stores blood from the pulmonary veins, resulting in atrial wall lengthening and corresponding positive strain values. In the conduit phase, occurring from mitral valve opening through early diastolic filling until late diastole, the LA passively transfers blood into the LV during early diastole. Subsequently, the conduit phase is characterized by substantial volumetric and strain changes, primarily involving passive flow into the ventricle. Finally, the contraction phase, beginning with active atrial contraction and ending at mitral valve closure, is marked by active atrial contraction that augments LV filling, generating further negative strain values due to myocardial shortening (Figure 1) (50, 52). Each of these phases reflects the dynamic interplay between atrial and ventricular mechanics. Specifically, LA reservoir strain reflects relaxation and compliance, influenced by LV systolic function through the descent of the LV base. The conduit function is influenced by LV diastolic properties, including relaxation and chamber stiffness, whereas the LA booster pump function depends on intrinsic atrial contractility and LV end-diastolic pressure and compliance (50). To ensure reproducibility, ventricular end-diastole is recommended as the zero-baseline reference point for LA strain curves, regardless of rhythm status (53).

Several studies have demonstrated that LA strain analysis significantly contributes to the early detection of diastolic dysfunction by providing a sensitive and non-invasive assessment of atrial performance (54, 55). Phasic LA strain parameters have been shown to predict worsening diastolic function over time more accurately than traditional echocardiographic parameters such as LA volume index (LAVi) (54, 56). LA strain also bears the potential to predict the occurrence of atrial fibrillation, providing incremental value for thromboembolic risk assessment beyond the CHA_2DS_2-VASc score (57-59). Nevertheless, despite growing recognition of the role of LA mechanics in diastolic function, data remain limited regarding the long-term prognostic value of LA longitudinal strain and its additive contribution beyond established LV function metrics in low-risk populations.

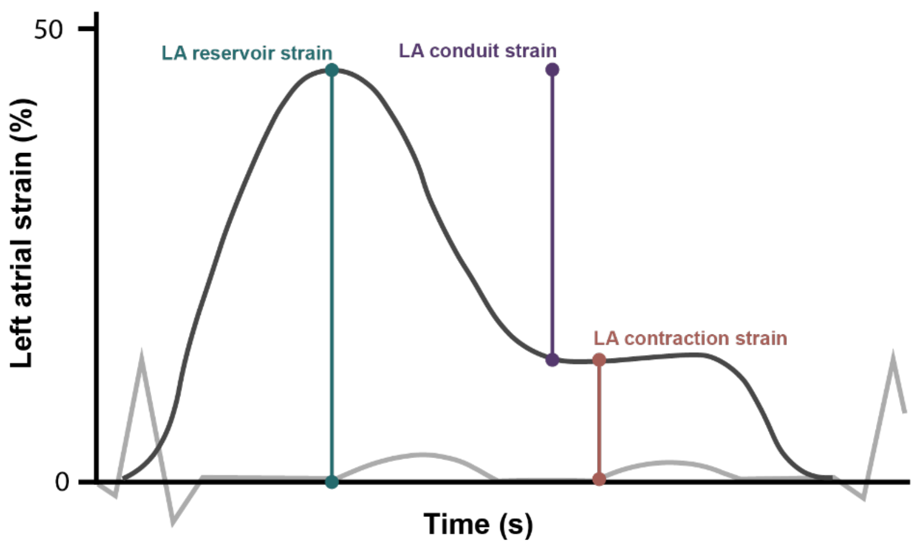

Figure 1*. Schematic illustration of strain-time curve synchronized with an electrocardiogram, depicting phasic left atrial strain indices. LA – left atrial.*

1.2.1.3 Myocardial work

Novel echocardiographic techniques, such as non-invasive LV pressure-strain loop–derived MW analysis, offer advanced insights into myocardial contractility that extend beyond conventional measures like LVEF and GLS by incorporating afterload into the evaluation of systolic performance (37, 38). To enable this, Russell et al. introduced an innovative approach to quantify MW by analysing the LV pressure-strain loop, which integrates longitudinal strain obtained through STE and estimated LV pressure curves, derived non-invasively from brachial artery cuff measurements performed at rest in the supine position prior to imaging (Figure 2).

To derive MW indices, key valvular events, namely, mitral valve closure and opening, as well as aortic valve opening and closure, should be precisely identified, corresponding to the isovolumetric contraction, ejection, isovolumetric relaxation, and diastolic filling phases of the cardiac cycle. Then, the global myocardial work index (GWI), representing the area within the pressure-strain loop, can be calculated by integrating instantaneous power over time from mitral valve closure to opening. Global constructive myocardial work (GCW) measures myocardial shortening during systole and lengthening during isovolumetric relaxation, representing work that contributes to effective LV ejection. Conversely, global wasted myocardial work (GWW) quantifies work that does not contribute effectively to LV ejection during systole, specifically lengthening during systole and shortening during isovolumetric relaxation. Lastly, global myocardial work efficiency (GWE), calculated as GCW/ (GCW + GWW), reflects the percentage of effective myocardial work relative to total work performed. Due to its ability to integrate myocardial deformation and loading conditions, MW analysis has gained increasing interest for its potential to improve functional assessment and risk stratification across various cardiovascular diseases; however, its prognostic utility in more nuanced subgroups within low-risk populations remains understudied (60-62).

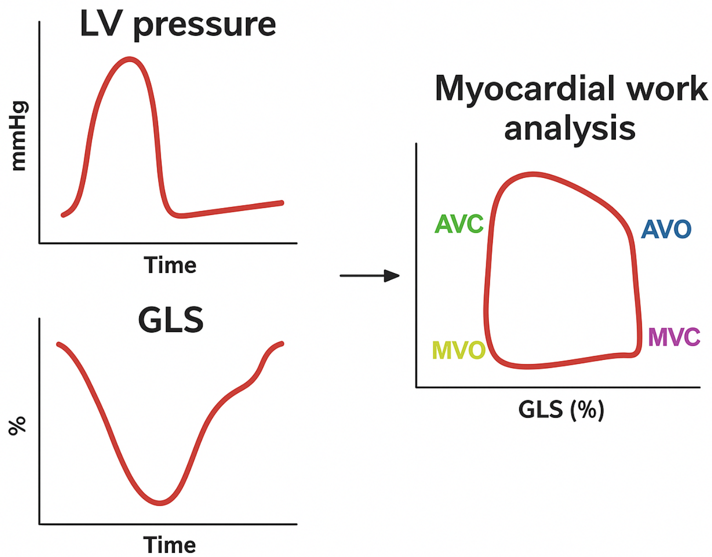

Figure 2. *Schematic workflow of myocardial work analysis. AVC, aortic valve closure; AVO, aortic valve opening, GLS, global longitudinal strain; LV, left ventricle; MVC, mitral valve closure, MVO, mitral valve opening. (Figure is based on illustration from (63)).*

2 Objectives

2.2 Investigation of the long-term prognostic importance of peak atrial longitudinal strain in a community-based screening sample comprising elderly individuals

Left ventricular diastolic dysfunction frequently precedes systolic dysfunction and is associated with comparable adverse long-term outcomes. Thus, the assessment of LV diastolic function along with LA function may offer more sensitive biomarkers to detect early dysfunction and predict long-term prognosis. Despite the well-known importance of LA mechanics in diastolic function evaluation, data are scarce regarding the long-term prognostic power of LA longitudinal strain and its potential added value on top of LV function indices. Accordingly, our aim was to determine the long-term prognostic importance of STE-derived peak atrial longitudinal strain (PALS) in a community-based screening sample comprising elderly individuals.

2.2 Evaluating the impact of overweight and obesity on myocardial work measures and assessing their prognostic power in a low-risk, community-based cohort

Although both LVEF and GLS are sensitive indicators of LV systolic function, both are notably affected by various factors, including loading conditions and heart rate. In contrast, MW provides insights into LV contractility that extend beyond more traditional measures, as it accounts for afterload, allowing a more accurate assessment of systolic performance. Accordingly, our objective was to evaluate the impact of overweight and obesity on myocardial work measures and to assess their prognostic power in a low-risk, community-based cohort.

3 Methods

3.2 Study sample

The Budakalász Study is a cross-sectional, voluntary screening program conducted between spring 2011 and January 2014, involving adults from the Central Hungarian region, aiming to collect information on their health state and cardiovascular risk profile and to discover new cardiovascular risk factors (64). Study procedures included questionnaires, non-invasive tests (anthropometry, echocardiography, carotid duplex scan, blood pressure measurement, ankle-brachial index), and venous blood sample collection for laboratory tests. Females over 40 years of age and males over 35 years of age were invited to participate in the cardiac computed tomography (CT) examinations. The individuals who participated in the aforementioned comprehensive screening program served as the study population and provided the foundation for the investigations presented in this thesis.

Considering the first study, to allow a comprehensive cardiovascular risk assessment in the elderly, the inclusion criteria included (1) the availability of transthoracic echocardiography, (2) the availability of carotid IMT measurement, and (3) the availability of the Agatston score. Patients with inadequate image quality for LV and LA longitudinal strain calculation by speckle-tracking analysis were excluded. In our second study, assessing the prognostic value of MW indices required the availability of transthoracic echocardiography, whereas the exclusion criteria were absence of apical four-chamber view loops, poor visualization of more than one LV segment in the apical four-chamber view, or suboptimal tracking quality as determined by an expert reader.

All participants provided written informed consent to study procedures. Both studies were in accordance with the Declaration of Helsinki and approved by the Medical Research Council (ETT-TUKEB No. 13687–0/2011-EKU).

3.2 General medical examination

As a part of the medical examination, complete medical history was obtained, with special emphasis given to cardiovascular diseases, as well as lifestyle factors (alcohol consumption, smoking, physical activity), family history, and medications. Blood samples were taken for laboratory analysis. Body weight and height were measured; then, body mass index (BMI) and body surface area (BSA) were calculated. A 12-lead electrocardiography (ECG) was also recorded (64). Blood pressure was measured using validated equipment in a supine position on both arms following 20 minutes of rest. For clinical characterization, individuals were classified as having hypertension, hyperlipidaemia, or diabetes mellitus if these conditions had been previously diagnosed or were under treatment, based on medical history. Coronary artery disease was defined as a history of myocardial infarction, previous coronary artery bypass grafting (CABG), or percutaneous coronary intervention (PCI). Using the Framingham risk score, we calculated the individual's 10-year risk of manifesting clinical cardiovascular disease (65).

3.2 Carotid duplex scan

A duplex scan of both carotid arteries was performed (Vivid i ultrasound system, 12L-RS linear probe, GE Healthcare, Horten, Norway), which was post-processed offline (GE EchoPAC) to measure carotid IMT according to the recommendations of the 2012 Mannheim Consensus. Additionally, a detailed description of the carotid plaques (if any) was performed (66). Importantly, these measurements were examined and reported exclusively in a subset of participants included in the first sub-study.

3.2 Cardiac CT

Females over 40 years of age and males over 35 years of age were offered to have a cardiac CT scan, which was performed on a 256-slice CT machine (Brilliance iCT, Philips Healthcare, Best, The Netherlands) and were exposed to a radiation dose of 0.5 mSv or less. Quantitative analysis of coronary calcification on the axial images was performed using a commercially available software (Calcium scoring, Heartbeat-CS, Philips), and the Agatston score was calculated and reported as 0 or non-0 for each patient only from the first sub-study (67).

3.2 Echocardiographic assessment

Using a commercially available ultrasound system (Vivid i, 3Sc-RS transducer), three experienced echocardiographers obtained all echocardiograms. All participants, including both studies, underwent a standard focused protocol comprising 2D imaging and tissue doppler imaging (TDI). The acquired images were analysed offline by two experienced investigators blinded to outcomes and clinical data using commercially available software packages (AutoStrain LV and AutoStrain LA, TomTec Imaging Systems, Unterschleißheim, Germany, and Ultrasound Workspace, Philips Medical Systems, The Netherlands).

3.5.1 Conventional echocardiography

LV internal diameters, wall thicknesses, and relative wall thickness were measured using the 2D-guided linear method. End-diastolic LV dimensions were used to calculate LV mass by an anatomically validated formula according to the recommendations of the American Society of Echocardiography (34). Specifically, in the first study, LV end-diastolic volume (EDV), end-systolic volume (ESV), and their BSA-indexed values, along with LVEF, were measured using the monoplane or the biplane Simpson's method. In both studies, left atrial end-systolic volume (LAV) was measured using the Simpson's method in the apical four-chamber view and was indexed to BSA to calculate LAVi (34). Mitral inflow was assessed using pulsed-wave Doppler between the tips of the mitral leaflets in the apical four-chamber view. Peak early (E) and late (A) diastolic inflow velocities were measured and used to determine the E/A ratio. Furthermore, the deceleration time (DT) of the E-wave was measured. From the TDI recordings, we measured systolic (s′), early diastolic (e′), and late diastolic (a′) velocities of the mitral lateral and septal annulus. We calculated the E/e′ ratio by dividing trans-mitral E velocity by e′ averaged from these sites. Concerning the right heart, right ventricular basal short-axis diameter (RVd) and tricuspid annular plane systolic excursion (TAPSE) were also measured. Right atrial end-systolic volume (RAV) was measured using the Simpson's method in the apical four-chamber view and was indexed to BSA to calculate RAVi.

3.5.2 Speckle-tracking echocardiography

In the first study, a dedicated, vendor-independent speckle-tracking software package (AutoStrain LV and AutoStrain LA, TomTec Imaging Systems, Unterschleißheim, Germany) was used to analyse LV and LA deformation using the apical four-chamber view. To avoid further patient dropout due to image quality, no attempt was made to analyse apical two-chamber and long-axis views. The primary measurements of interest included the LV GLS (average of six LV segments) and peak atrial longitudinal strain (PALS) referring to the reservoir function of the LA (43, 50). The segmental peak negative values (longitudinal shortening) were used to calculate LV GLS. The peak positive value of the LA strain curve (lengthening in systole — reservoir function) was used to calculate PALS, and the late diastolic peak or plateau before P wave was used to calculate peak atrial contraction strain (PACS). The ventricular end-diastole was used as the reference time point for LA strain analysis. To assess the discriminatory power of PALS, a conventionally accepted cut-off value of 39% was used (51).

3.5.3 Myocardial Work analysis

Regarding the second study, similarly, a commercially available, validated, vendor-independent speckle-tracking software package (AutoStrain LV,198 Philips Ultrasound Workspace, Philips Medical Systems, The Netherlands) was used to quantify LVGLS and LV EDV, ESV, and LVEF. Similarly, to minimize patient dropout due to suboptimal image quality, volumetric indices and LVEF were measured only on apical four-chamber views, and LVGLS was calculated as the average peak negative strain of the six corresponding LV segments (43). In instances of suboptimal ECG or 2D echocardiographic image quality or low tracking fidelity, manual corrections to cardiac cycle events or the endocardial contours were performed as necessary.

Then, LVGLS segmental curves were subsequently exported as text files for further analysis using a custom-developed software dedicated to quantifying myocardial work metrics.

When performing MW analysis in the second study, principles previously established by Russell et al. were followed (38, 68). First, the peak systolic blood pressure values were obtained by performing and averaging brachial artery cuff pressure measurements on both arms. It was considered equivalent to the peak systolic pressure of the left ventricle and was assumed to be uniformly distributed across the ventricle. Then, the custom-developed software automatically reconstructed the LV pressure curve by adjusting the previously published LV reference curve according to the non-invasively obtained peak arterial pressure (38). To determine the timing of valvular events, pulsed-wave TDI recordings of the mitral lateral annulus were used. To approximate the opening and closure of the aortic and mitral valves, the stages of the cardiac cycle were measured on the recordings as isovolumic contraction time (IVCT), ejection time (ET), isovolumic relaxation time (IVRT), and filling time (FT). Utilizing these temporal reference points, we proportionally segmented the strain curves into four sections, each corresponding to a phase of the cardiac cycle, and each section of the given strain curve was matched with the corresponding section of the estimated pressure curve. Lastly, the four sections of the recordings were concatenated, and then, using our dedicated software, pressure–strain loops were plotted to enable myocardial work analysis.

Myocardial work was quantified by calculating the segmental shortening rate, derived from the differentiation of the strain curve, and multiplying this value by the instantaneous LV pressure. Subsequently, each MW metric, namely GWI, GCW, GWW, and GWE, was calculated as outlined previously.

3.2 Study outcomes

For both studies, follow-up data (status [dead or alive], date of death) were obtained from Hungary’s National Health Insurance Database. The primary endpoint for both studies was all-cause mortality.

3.2 Statistical analysis

Statistical analysis was performed using dedicated software (SPSS v22, IBM, Armonk, NY, USA). Continuous variables are expressed as mean ± standard deviation (SD), whereas categorical variables are reported as frequencies and percentages. After the verification of normal distribution of variables using the Shapiro–Wilk test, the clinical and echocardiographic characteristics were compared with unpaired Student's *t* test or Mann–Whitney *U* test for continuous variables, and chi-squared or Fisher's exact test for categorical variables, as appropriate. Cox proportional hazards models were used to compute HRs with 95% CIs. Covariates included in multivariable models were selected based on clinical relevance and intergroup differences. Collinearity of variables was tested at each multivariable model by the variance inflation factor (excessive if the variance inflation factor > 3). In the first study, receiver operating characteristic (ROC) curves were generated to assess the discriminatory power of PALS for the endpoint. Youden's index was used to identify the optimal cut-off point; then, this value or the conventionally used 39% value was used to dichotomize the study population. Outcomes of the dichotomized groups were visualized on Kaplan–Meier curves and compared by log-rank test. In the second study, the previously established lower limits of normal value (GWI value of 1292 mmHg%) (69) were used to dichotomize the study population. Outcomes of the dichotomized groups were visualized on Kaplan–Meier curves and compared by log-rank test. The prognostic performance of the established GWI cutoff was further evaluated using multivariable Cox proportional hazard models, including covariates of clinical relevance and intergroup differences, as described above. In both studies, a two-sided *P*-value of 0.05 was considered statistically significant.

4 Results

4.2 Investigation of the long-term prognostic importance of peak atrial longitudinal strain in a community-based screening sample comprising elderly individuals

4.1.1 Baseline demographic and clinical characteristics

Three hundred and fourteen individuals were retrospectively identified with a previous 2D transthoracic echocardiographic examination available. During a median follow-up of 9.5 [interquartile range: 9.1–9.9] years, 39 subjects met the primary endpoint of all-cause mortality (33).

Baseline demographic and clinical characteristics are summarized in Table 1. Subjects with adverse outcomes were significantly older, whereas there was no difference in sex within the study groups. The BMI values of subjects with adverse outcomes were significantly higher, while the BSA values remained similar in the two groups. Subjects who experienced adverse outcomes had higher systolic blood pressures, whereas there was no difference in diastolic blood pressure and heart rate in the study groups. Concerning cardiovascular risk factors, there were no significant differences between groups (Table 1). Regarding laboratory parameters, total cholesterol, low-density lipoprotein (LDL) cholesterol, and estimated glomerular filtration rate (eGFR) levels were significantly lower, whereas pro-hormone B-type natriuretic peptide (ProBNP), serum creatinine, and haemoglobin A1c (HbA1c) levels were significantly higher among subjects who met the endpoint. On the other hand, high-density lipoprotein (HDL)-cholesterol, triglycerides, and serum glucose levels did not show a difference between the study groups (Table 1) (33).

Table 1. Demographic and clinical characteristics

	Overall (n=314)	**Alive (n = 275)**	**Deceased (n = 39)**	**p value**
Baseline demographic characteristics				
Age (years)	61.5 ± 10.7	60.5 ± 10.3	68.6 ± 10.8	**<0.001**
Female, n (%)	182 (57.9)	165 (60.0)	17 (43.6)	0.052
Clinical characteristics				

BSA, m^2	1.89 ± 0.22	1.88 ± 0.22	1.95 ± 0.18	0.064
BMI, kg/m^2	28.5 ± 4.9	28.1 ± 4.9	30.9 ± 4.7	**<0.001**
Systolic blood pressure, mmHg	137.9 ± 18.9	136.8 ± 18.6	145.7 ± 19.4	**0.006**
Diastolic blood pressure, mmHg	78.9 ± 11.0	79.1 ± 11.0	78.3 ± 10.9	0.679
Heart rate, bpm	69.2 ± 10.3	68.9 ± 9.9	71.4 ± 12.3	0.153
Risk factors and medical history				
Smoking history, n (%)	130 (41.4)	108 (39.2)	22 (56.4)	**0.042**
Hypertension, n (%)	183 (58.0)	165 (60.0)	18 (46.2)	0.101
Diabetes, n (%)	55 (17.5)	49 (17.8)	6(15.4)	0.708
Arrhythmia, n (%)	40 (12.7)	33 (12.0)	7 (17.9)	0.297
Previous MI, n (%)	13(4.1)	13 (4.7)	0 (0)	0.165
Previous PCI, n (%)	3 (0.9)	3 (1.1)	0 (0)	0.512
Previous CABG, n (%)	1 (0.3)	1 (0.4)	0 (0)	0.706
Previous stroke, n (%)	14 (4.5)	13 (4.7)	1 (2.6)	0.540
Pulmonary disease, n (%)	21 (6.7)	17 (6.2)	4 (10.3)	0.194
Framingham risk score	19.4 ± 12.3	17.9 ± 11.5	29.9 ± 12.6	**<0.001**
Agatston score (non-0), n (%)	204 (64.9)	170 (61.8)	34 (87.2)	**0.002**
IMT, mm	0.73 ± 0.14	0.71 ± 0.14	0.80 ± 0.12	**0.001**
Laboratory parameters				
Total cholesterol, mmol/L	5.7 ± 1.2	5.7 ± 1.1	5.3 ± 1.3	**0.027**
HDL cholesterol, mmol/L	1.5 ± 0.5	1.5 ± 0.5	1.5 ± 0.5	0.575
LDL cholesterol, mmol/L	3.5 ± 1.0	3.6 ± 0.9	3.2 ± 1.3	**0.030**
Triglycerides, mmol/L	2.3 ± 1.4	2.3 ± 1.4	2.2 ± 1.4	0.737
Glucose, mmol/L	6.2 ± 1.9	6.1 ± 1.7	6.6 ± 2.5	0.140
ProBNP, pmol/L	127.2 ± 181.9	104.1 ± 114.5	293.0 ± 385.6	**<0.001**
Serum Creatinine, µmol/L	77.2 ± 16.8	76.5 ± 16.2	82.2 ± 19.7	**0.045**
eGFR, ml/min	82.1 ± 16.4	83.0 ± 15.9	75.8 ± 18.5	**0.011**
HbA1c, %	5.9 ± 0.8	5.8 ± 0.7	6.3 ± 1.2	**0.001**

Continuous variables are presented as means ± SD, categorical variables are reported as frequencies (%). BMI, body mass index; BSA, body surface area; CABG, coronary artery bypass grafting; eGFR, estimated glomerular filtration ratio; HbA1C, haemoglobin A1C; HDL, high density lipoprotein; IMT, carotid intima-media thickness; LDL, low density lipoprotein; MI, myocardial infarction; PCI, percutaneous coronary intervention; ProBNP, pro-hormone B-type natriuretic peptide.

4.1.2 Conventional 2D and speckle-tracking echocardiographic parameters

Conventional 2D echocardiographic parameters of the study population are shown in Table 2. LV end-diastolic internal diameter and calculated LV mass index (LVMi) values were significantly higher in subjects with adverse outcome, in contrast to wall thickness and relative wall thickness (RWT) values, which did not differ between the two groups. Subjects who experienced adverse outcomes showed significantly higher values of indexed LV ESV and indexed EDV. However, LVEF did not show a difference between study groups. Regarding diastolic function, subjects who met the endpoint demonstrated significantly higher mitral A-wave velocity and lower E/A ratios along with a significantly longer deceleration time, whereas E-wave velocity did not show a difference. Furthermore, mitral annular early diastolic velocities were significantly lower, whereas the average E/e′ ratio was higher in subjects with adverse outcome. 2D LAVi was significantly higher among subjects who met the endpoint. Regarding the right heart, RV basal diameter along with TAPSE and 2D RAVi did not show any difference between the two study groups (Table 2).

Regarding speckle-tracking echocardiography-derived data, subjects with adverse outcome, showed lower LVGLS values compared to those without. Concerning LA mechanics, PALS showed significantly lower values in subjects who met the endpoint. Conversely, PACS did not show a difference between the two study groups (Table 2) (33).

Table 2. Echocardiographic parameters of study population

	Overall (n = 314)	Alive (n = 275)	Deceased (n = 39)	p value
2D conventional echocardiographic data				
LVIDd, mm	47.9 ± 4.7	47.7 ± 4.5	50.1 ± 5.9	**0.003**
IVSd, mm	9.9 ± 1.8	9.9 ± 1.8	10.3 ± 1.9	0.221
PWd, mm	9.7 ± 1.6	9.6 ± 1.6	10.1 ± 1.6	0.078
RWT, %	0.41± 0.08	0.41 ± 0.07	0.41 ± 0.09	0.636
LV Mi, g/m^2	88.7 ± 22.8	87.7 ± 22.7	96.0 ± 23.0	**0.042**
LV ESVi, ml/m^2	38.6 ± 13.1	37.9 ± 12.1	43.3 ± 17.7	**0.018**
LV EDVi, ml/m^2	79.9 ± 22.1	78.9 ± 21.2	87.5 ± 26.3	**0.021**
EF, %	51.9 ± 6.3	52.1 ± 6.2	51.1 ± 7.0	0.347

E, cm/s	75.7 ± 18.9	75.3 ± 16.7	78.3 ± 30.2	0.358
A, cm/s	75.5 ± 22.9	74.1 ± 22.5	86.2 ± 22.3	**0.002**
E/A	1.09 ± 0.48	1.11 ± 0.47	0.94 ± 0.49	**0.039**
DT (ms)	211.9 ± 62.7	208.8 ± 59.9	234.7 ± 77.0	**0.017**
Mitral lateral s', cm/s	8.9 ± 2.5	8.9 ± 2.4	8.6 ± 3.0	0.567
Mitral lateral e', cm/s	10.3 ± 3.3	10.5 ± 3.3	8.7 ± 2.2	**0.002**
Mitral lateral a', cm/s	10.7 ± 3.2	10.7 ± 3.1	11.1 ± 4.3	0.463
Mitral medial s', cm/s	8.36 ± 1.9	8.39 ± 1.8	8.1 ± 1.9	0.427
Mitral medial e', cm/s	8.8 ± 2.9	9.1 ± 2.9	7.3 ± 2.5	**<0.001**
Mitral medial a', cm/s	11.0 ± 2.7	11.01 ± 2.6	10.9 ± 3.2	0.884
E/e' average	8.4 ± 3.1	8.11 ± 2.9	10.0 ± 3.9	**<0.001**
LAVi, ml/m^2	33.2 ±10.4	32.3 ± 9.7	38.9 ± 12.7	**<0.001**
RVd, mm	35.2 ± 5.8	35.1 ± 5.8	35.6 ± 5.5	0.623
TAPSE, mm	24.7 ± 4.2	24.7 ± 4.0	24.3 ± 5.0	0.595
RAVi, ml/m^2	22.5 ± 11.6	22.1 ± 11.6	25.7 ± 11.2	0.069
Speckle tracking echocardiography data				
LVGLS, %	-20.5 ± 3.7	-20.6 ± 3.5	-19.2 ± 4.3	**0.022**
PALS, %	40.6 ± 14.2	41.8 ± 14.2	32.3 ± 11.9	**<0.001**
PACS, %	18.8 ± 8.7	18.9 ± 8.8	17.2 ± 7.9	0.225

Continuous variables are presented as means ± SD, categorical variables are reported as frequencies (%). A, atrial contraction; a', peak late (atrial) diastolic annular velocity; DT, deceleration time; E, early diastolic filling; e', early diastolic annular velocity; EDVi, end diastolic volume index; EF, ejection fraction; ESVi, end-systolic volume index; IVSd, inter-ventricular septal diameter; LAVi, left atrial volume index; LV, left ventricle; LVGLS, left ventricular global longitudinal strain; LVIDd, left ventricular internal diameter at end-diastole; LV Mi, left ventricular mass index; PWd, posterior wall diameter; PACS, peak atrial contraction strain; PALS, peak atrial longitudinal strain; RAVi, right atrial volume index; RVd, right ventricle diameter; RWT, relative wall thickness; s', systolic annular velocity; TAPSE, tricuspid annular plane systolic excursion

4.1.3 Prognostic value and discriminatory power of PALS

Including significant variables identified at the univariable Cox regression analysis, multivariable Cox regression analysis was performed, and the results are summarized in Table 3. In order to identify independent predictors of outcomes and to determine the prognostic value of PALS, three multivariable Cox regression models were built, including Framingham risk score and PALS in each model. In Model 1, comprising Framingham risk score, PALS, and LVGLS, PALS was found to be independently associated with the adverse outcome along with Framingham risk score. In Model 2, consisting of Framingham risk score, PALS, and carotid IMT, all three variables were independently associated with all-cause mortality. Concerning Model 3, which comprised Framingham risk score, PALS, and Agatston score, only PALS and Framingham risk score were found to be independently associated with the adverse outcome (Table 3) (33).

Using the conventional cut-off value of 39%, PALS was able to discriminate between a high-risk and a low-risk group in terms of all-cause mortality. As depicted by Kaplan–Meier curves, in subjects with lower PALS values, the risk of all-cause mortality was almost 2.5 times higher than in subjects with PALS values above 39% (HR: 2.499 [95% CI: 1.334–4.682], $p < 0.05$) (Figure 3, Figure 4).

ROC analysis was also performed to assess the discriminatory power of PALS with regard to the endpoint. The area under the ROC curve is shown in Figure 5. Using Youden's index, we calculated the optimal cut-off value of 32.6% with a sensitivity of 56.4% and specificity of 75.3% (Figure 5). When using this cut-off, in subjects with lower PALS values, the risk of all-cause mortality was more than three times higher than in subjects with PALS values above 32.6% (HR: 3.424 [95% CI: 1.694–6.919], $p < 0.001$) (Figure 6) (33).

Table 3. Independent predictors of all-cause mortality identified using multivariable Cox regression

	Multivariable Cox regression					
	Model 1		Model 2		Model 3	
	HR [95% CI]	**P**	**HR [95% CI]**	**P**	**HR [95% CI]**	**P**
Framingham risk score	1.056 [1.032 - 1.081]	**<0.001**	1.042 [1.015-1.071]	**0.003**	1.046 [1.020-1.073]	**<0.001**
PALS	0.967 [0.939 -0.995]	**0.023**	0.954 [0.924-0.985]	**0.004**	0.967 [0.941-0.993]	**0.012**
LVGLS	1.032 [0.938-1.134]	0.521	-		-	
IMT	-		14.62[1.036-206.24]	**0.047**	-	
Agatston score (non 0)	-		-		2.536 [0.742-8.669]	0.138

CI, confidence interval; HR, hazard ratio; IMT, carotid intima-media thickness; LVGLS, left ventricular global longitudinal strain; PALS, peak atrial longitudinal strain

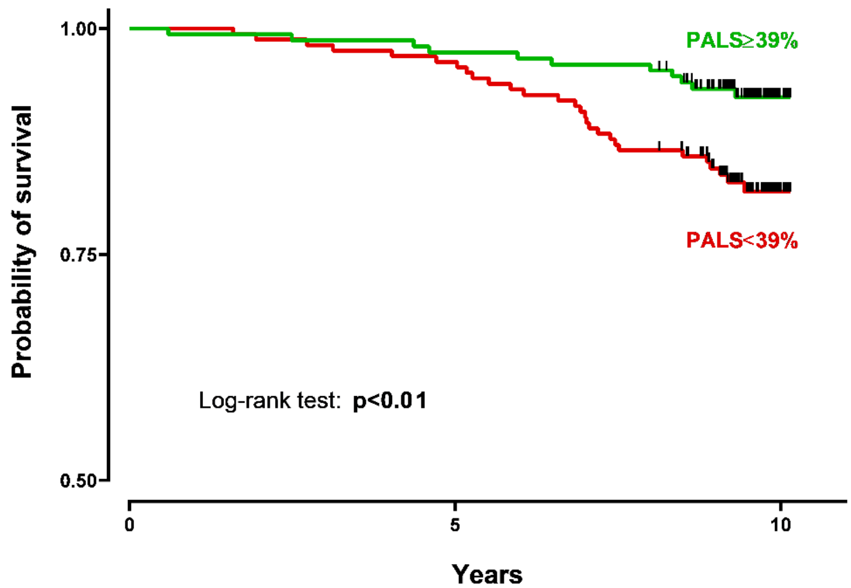

Figure 3. *Kaplan-Meier survival curves using a standard cut-off value of 39%. PALS, peak atrial longitudinal strain.*

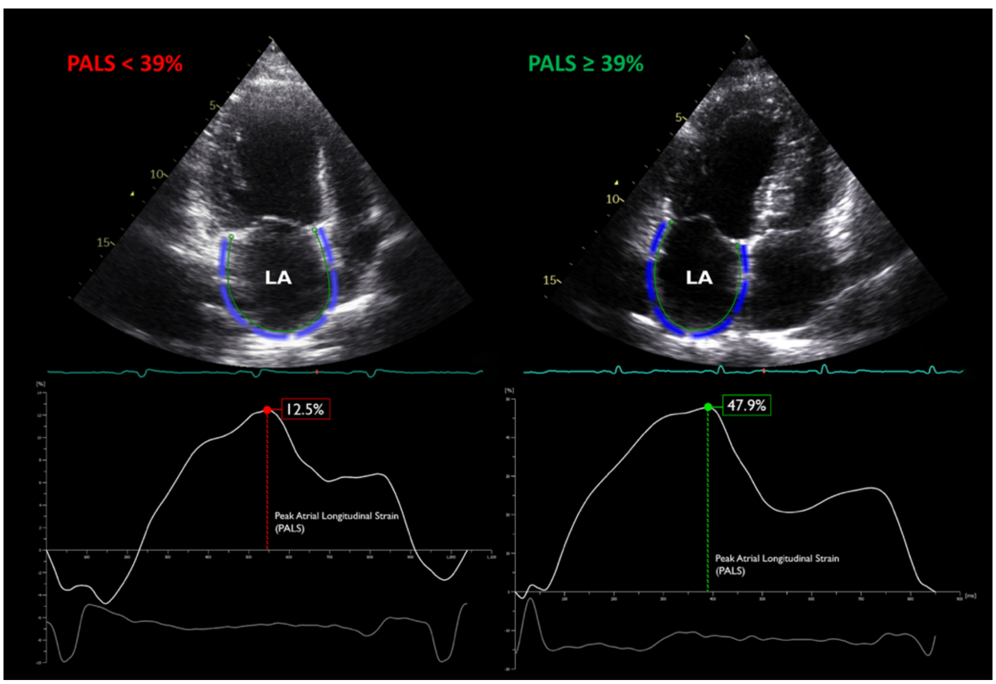

Figure 4. *Representative cases of subjects below (indicated with red) and above 39% (indicated with green) of peak atrial longitudinal strain (PALS). Subject with 12.6% PALS met the primary endpoint during the follow-up period. The blue contour on the 2D echocardiographic image depicts left atrial (LA) endocardial border at end-systole (33).*

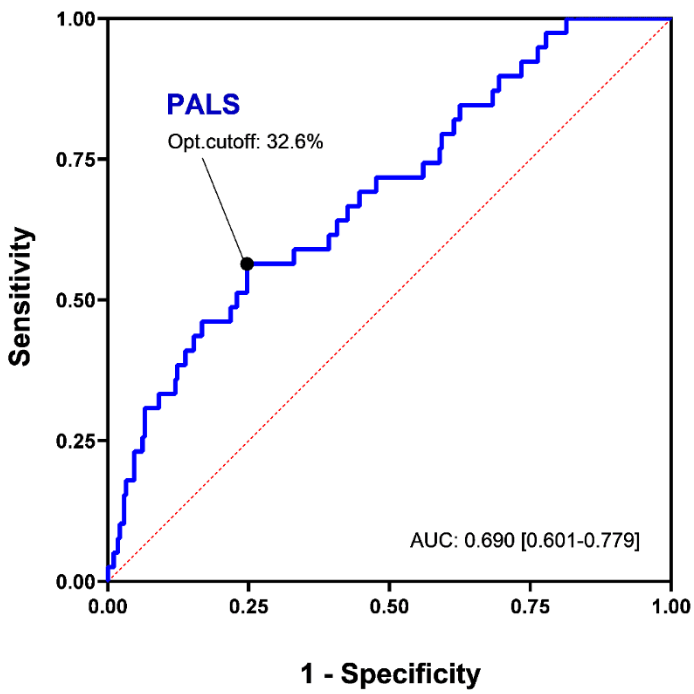

Figure 5. *Receiver operating characteristic curve illustrating the discriminatory power of PALS with regard to the endpoint. AUC, area under the curve; PALS, peak atrial longitudinal strain (33).*

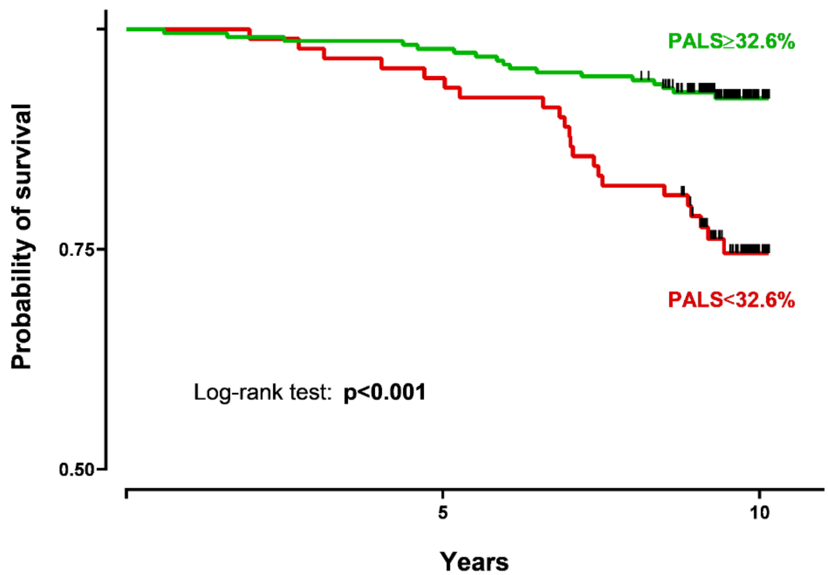

Figure 6. *Kaplan-Meier survival curves based on the optimal cut-off value (32.6%) of PALS assessed with receiver operating characteristic analysis. PALS, peak atrial longitudinal strain (33).*

4.2 Evaluating the impact of overweight and obesity on myocardial work measures and assessing their prognostic power in a low-risk, community-based cohort

4.2.1 Baseline demographic and clinical characteristics according to primary outcome

A total of 1330 individuals with 2D transthoracic echocardiographic examinations were retrospectively identified. Over a median follow-up period of 11 years, 138 participants reached the primary endpoint of all-cause mortality (70).

Baseline demographic and clinical characteristics are outlined in Table 4. Individuals with adverse outcomes were significantly older, and there was a significant male predominance in the deceased group (57.2%). Subjects with adverse events had significantly higher BMI values, while BSA values were comparable across groups. Higher systolic and lower diastolic blood pressure was observed among those with adverse outcomes, with no significant difference in heart rate. Regarding cardiovascular risk factors, the most common was hypertension, affecting 47.0 % of the participants, followed by a history of smoking (42%) and diabetes (13%). In terms of laboratory findings, there were no differences between the groups (Table 4) (70).

Table 4. Demographic and clinical characteristics of the study samples according to primary outcome

	Overall (n=1330)	**Alive (n =1192)**	**Deceased (n =138)**	**p-value**
Baseline demographic characteristics				
Age (years)	53.41±14.70	51.90±13.87	66.43±15.28	**<0.001**
Female, n (%)	772 (58.05)	713 (59.82)	59 (42.75)	**<0.001**
Clinical characteristics				
BSA, m^2	1.90±0.23	1.90±0.23	1.91±0.23	0.893
BMI, kg/m^2	27.79±5.01	27.65±5.02	29.03±4.78	**0.002**
Systolic blood pressure, mmHg	132.84±18.32	132.00±17.81	140.08±20.95	**<0.001**

Diastolic blood pressure, mmHg	79.40±9.65	79.62±9.57	77.52±10.16	**0.016**
Heart rate, bpm	68.06±9.85	67.96±9.89	68.91±9.49	0.286
Risk factors and medical history				
Smoking history, n (%)	557(41.88)	494 (41.44)	63 (45.65)	0.343
Hypertension, n (%)	625 (46.99)	560 (46.98)	65 (47.10)	0.978
Diabetes, n (%)	169 (12.71)	158 (13.26)	11 (7.97)	0.078
Arrhythmia n (%)	138 (10.38)	122 (10.23)	36 (18.85)	0.620
Previous MI, n (%)	39 (2.93)	38 (3.19)	1 (0.72)	0.104
Previous PCI, n (%)	24 (1.80)	23 (1.93)	1 (0.72)	0.314
Previous CABG, n (%)	12 (0.90)	11 (0.92)	1 (0.72)	0.054
Chronic heart failure, n (%)	83 (6.24)	81 (6.80)	2 (1.45)	**0.014**
Previous stroke, n (%)	62 (4.66)	58 (4.87)	4 (2.90)	0.299
Pulmonary disease, n (%)	97 (7.29)	84 (7.05)	13 (9.42)	0.310
Framingham risk score	15.32±13.09	15.45±13.13	14.19±12.65	0.287
Laboratory work				
Total cholesterol, mmol/L	5.48±1.13	5.46±1.14	5.54±1.05	0.523
HDL cholesterol, mmol/L	1.47±0.44	1.46±0.44	1.52±0.42	0.156
LDL cholesterol, mmol/L	3.37±0.97	3.37±0.98	3.41±0.90	0.674
Triglycerides, mmol/L	2.27±1.61	2.28±1.62	2.13±1.49	0.296
Glucose, mmol/L	5.98±1.52	6.00±1.56	5.77±1.08	0.087
ProBNP, pmol/L	126.19±319.66	130.38±335.82	90.13±97.83	0.165
Serum Creatinine, µmol/L	77.29±18.58	77.40±18.69	76.28±17.63	0.502
HBa1c, %	5.74±0.73	5.76±0.75	5.63±0.51	0.050

BMI, body mass index; BSA, body surface area; CABG, coronary artery bypass grafting; HBA1c, haemoglobin A1c; HDL, high density lipoprotein; LDL, low density lipoprotein; MI, myocardial infarction; PCI, percutaneous coronary intervention; ProBNP, pro-hormone B-type natriuretic peptide.

4.2.2 Conventional 2D and speckle-tracking echocardiography-derived parameters according to primary outcome

The conventional 2D echocardiographic parameters are presented in Table 5. Participants with adverse outcomes showed marked LV remodelling, with larger internal diameters and higher values of LVMi, EDVi, and ESVi, while LVEF was similar across groups. In terms of diastolic function, patients with adverse outcomes had significantly higher mitral A-wave velocity and lower E-wave velocity, along with a lower E/A ratio and prolonged DT. Mitral annular early diastolic velocities were lower in the adverse outcome group, and the average E/e′ ratio was higher. Additionally, LAVi was higher in those who met the endpoint. Regarding the right heart, only RAVi was higher in the deceased group. STE and MW analysis-derived metrics revealed significantly lower LVGLS and GWI in the deceased group, along with higher GWW and lower GWE, while GCW did not differ (Table 5) (70).

Table 5. Echocardiographic parameters of study population according to primary outcome

	Overall (n = 1330)	Alive (n = 1192)	Deceased (n = 138)	p-value
2D conventional echocardiographic data				
LVIDd, mm	48.29±4.79	48.14±4.72	49.71±5.22	**<0.001**
IVSd, mm	9.94±1.75	9.84±1.67	10.88±2.13	**<0.001**
PWd, mm	9.37±1.51	9.31±1.46	9.91±1.81	**<0.001**
RWT, %	0.44±0.13	0.44±0.13	0.46±0.16	**0.030**
LVMi, g/m^2	87.50±21.52	85.87±20.04	102.42±28.06	**<0.001**
LV ESVi, ml/m^2	20.63±4.98	20.46±4.89	22.19±5.52	**<0.001**
LV EDVi, ml/m^2	59.15±11.09	58.80±11.08	62.25±10.73	**<0.001**
EF, %	65.11±5.21	65.19±5.12	64.33±5.92	0.065
E, cm/s	76.40±17.69	76.74±16.88	73.36±23.51	**0.037**
A, cm/s	68.88±21.00	67.58±20.36	80.28±23.11	**<0.001**
E/A	1.22±0.51	1.24±0.50	1.02±0.58	**<0.001**
DT (ms)	201.89±58.58	198.51±55.87	231.61±72.23	**<0.001**
Mitral lateral s', cm/s	9.88±2.69	9.95±2.66	9.26±2.87	**0.004**
Mitral lateral e', cm/s	12.31±4.17	12.58±4.10	10.00±4.01	**<0.001**

Mitral lateral a', cm/s	10.39±3.18	10.28±3.10	11.30±3.67	**<0.001**
Mitral medial s', cm/s	8.58±1.79	8.64±1.75	8.08±2.01	**<0.001**
Mitral medial e', cm/s	9.80±3.38	10.02±3.34	7.88±3.06	**<0.001**
Mitral medial a', cm/s	10.46±2.42	10.46±2.37	10.53±2.79	0.725
E/e' average	7.47±2.59	7.28±2.32	9.12±3.95	**<0.001**
LAVi, ml/m^2	28.94±9.88	28.39±9.42	33.65±12.27	**<0.001**
RVd, mm	34.62±5.41	34.53±5.36	35.40±5.75	0.073
RAVi, ml/m^2	23.13±7.88	22.91±7.80	25.08±8.35	**0.003**
TAPSE, mm	23.85±4.04	23.82±3.99	24.10±4.40	0.457
Speckle tracking echocardiography data				
LVGLS, %	-19.94±3.49	-20.06±3.44	-18.85±3.79	**<0.001**
Myocardial work data				
GWI, mmHg%	2040.65±483.64	2051.02±473.57	1951.05±557.20	**0.021**
GCW, mmHg%	2194.21±472.40	2198.89±463.23	2153.85±545.48	0.289
GWW, mmHg%	144.97±104.14	142.48±102.50	166.51±115.55	**0.010**
GWE, %	93.72±4.27	93.84±4.18	92.68±4.87	**0.003**

A, atrial contraction; a', peak late (atrial) diastolic annular velocity; DT, deceleration time; E, early diastolic filling; e', early diastolic annular velocity; EDVi, end diastolic volume index; EF, ejection fraction; ESVi, end-systolic volume index; GCW, global constructive work; GLS, global longitudinal strain; GWE, global work efficiency; GWI, global work index; GWW, global wasted work; IVSd, inter-ventricular septal diameter; LAVi, left atrial volume index; LV, left ventricle; LVIDd, left ventricular internal diameter at end-diastole; LVMi, left ventricular mass index; PWd, posterior wall diameter; RAVi, right atrial volume index; RVd, right ventricle diameter; RWT, relative wall thickness; s', systolic annular velocity; TAPSE, tricuspid annular plane systolic excursion.

4.2.3 Baseline demographic and clinical characteristics according to body mass index

Based on BMI, the total cohort was divided into 3 weight groups. The normal weight group (n=405) was defined as BMI ≥18.5 and <25, the group with overweight (n=526) was defined as BMI ≥25 and <30, whereas the group with obesity (n=399) consisted of patients with BMI ≥30 as per WHO data (20). Table 6 summarizes the demographic and clinical characteristics of each weight group. Subjects in the normal weight group were younger and had a higher proportion of females. Compared to the groups with overweight and obesity, the normal weight group also exhibited significantly lower systolic and diastolic blood pressure. The all-cause mortality rate was higher among overweight and obese individuals compared to those in the normal weight group, and interestingly, it was comparable between the overweight and obese groups. Regarding cardiovascular risk factors, no significant differences were observed in terms of smoking status, hypertension, or diabetes. Additionally, laboratory parameters did not differ between groups (Table 6). Patients who met the endpoint vs those who did not, were also compared within the three weight groups. Interestingly, deceased patients among the normal weight and overweight groups had higher systolic blood pressures, whereas within the group with obesity, there was no difference between the alive and deceased subjects. Moreover, the alive and deceased groups did not differ in terms of cardiovascular risk factors (70).

Table 6. Demographic and clinical characteristics of the study samples according to BMI categories

	Overall	**Normal weight (n=405)**	**Overweight (n=526)**	**Obese (n=399)**	**p-value**
Baseline demographic characteristics					
Age (years)	53.41±14.70	46.7±15.0[bc]	54.7±14.5[ac]	58.5±11.8[ab]	**<0.001**
Female, n (%)	772 (58.05)	290 (71.60)[bc]	240 (45.63)[ac]	242 (39.35)[ab]	**<0.001**
Deceased, n (%)	138 (10.37)	37 (5.43)[bc]	67 (12.74)[a]	49 (12.28)[a]	**<0.001**
Clinical characteristics					
BSA, m^2	1.90±0.23	1.72±0.17[bc]	1.92±0.18[ac]	2.06±0.19[ab]	**<0.001**
BMI, kg/m^2	27.79±5.01	22.36±1.90[bc]	27.40±1.39[ac]	33.81±3.35[ab]	**<0.001**
Systolic blood pressure, mmHg	132.84±18.32	126.25±19.34[bc]	134.19±17.76[ac]	137.75±15.94[ab]	**<0.001**
Diastolic blood pressure, mmHg	79.40±9.65	77.13±10.06[bc]	79.24±9.07[ac]	81.92±9.38[ab]	**<0.001**
Heart rate, bpm	68.06±9.85	66.81±9.78[c]	67.57±9.83[c]	69.92±9.70[ab]	**<0.001**

Risk factors and medical history					
Smoking history, n (%)	557(41.88)	161 (39.85)	213 (40.49)	183 (48.86)	0.152
Hypertension, n (%)	625 (46.99)	177 (43.81)	256 (48.67)	192 (48.12)	0.279
Diabetes, n (%)	169 (12.71)	47 (11.63)	66 (12.55)	56 (14.04)	0.580
Arrhythmia n (%)	138 (10.38)	45 (11.14)	50 (9.51)	43 (10.78)	0.693
Previous MI, n (%)	39 (2.93)	10 (2.48)	9 (1.71)	20 (5.01)	**0.010**
Previous PCI, n (%)	24 (1.80)	6 (1.49)	12 (2.28)	6 (1.50)	0.572
Previous CABG, n (%)	12 (0.90)	6 (1.49)	4 (0.76)	2 (0.50)	0.308
Chronic heart failure, n (%)	83 (6.24)	29 (7.18)	33 (6.27)	21 (5.26)	0.538
Previous stroke, n (%)	62 (4.66)	15 (3.71)	32 (6.08)	15 (3.76)	0.138
Pulmonary disease, n (%)	97 (7.29)	23 (5.69)	41 (7.79)	33 (8.27)	0.313
Framingham risk score	15.32±13.09	14.51±12.49	15.51±13.28	15.90±13.42	0.294
Laboratory work					
Total cholesterol, mmol/L	5.49±1.14	5.56±1.13	5.48±1.15	5.41±1.09	0.186
HDL cholesterol, mmol/L	1.48±0.45	1.45±0.42	1.49±0.46	1.45±0.41	0.275
LDL cholesterol, mmol/L	3.37±0.97	3.45±0.95	3.36±0.99	3.30±0.96	0.099
Triglycerides, mmol/L	2.27±1.65	2.30±1.61	2.25±1.71	2.26±1.47	0.877
Glucose, mmol/L	5.96±1.51	6.04±1.66	5.92±1.35	6.00±1.58	0.732

ProBNP, pmol/L	133.13±421.99	132.23±436.91	118.44±206.93	130.22±301.04	0.776
Serum Creatinine, µmol/L	77.15±18.72	77.71±16.72	77.12±20.72	77.08±17.39	0.860
HBa1c, %	5.73±0.72	5.76±0.75	5.75±0.72	5.71±0.72	0.572

Continuous variables are presented as means ± SD, categorical variables are reported as frequencies (%); a: p < 0.05 vs. Normal weight, b: p < 0.05 vs. Overweight, c: p < 0.05 vs. Obese. BMI, body mass index; BSA, body surface area; CABG, coronary artery bypass grafting; HBa1c, haemoglobin A1C; HDL, high density lipoprotein; LDL, low density lipoprotein; MI, myocardial infarction; PCI, percutaneous coronary intervention; ProBNP, pro-hormone B-type natriuretic peptide.

4.2.4 Conventional 2D and speckle-tracking echocardiography-derived parameters according to BMI groups

Conventional 2D echocardiographic parameters of patients in the three weight groups are shown in Table 7 (70). Individuals in the obese group exhibited higher values of LV end-diastolic dimensions, and LVMi, whereas patients in the overweight groups had higher LV EDVi. Interestingly, LVEF was significantly lower in the normal group compared to the groups with overweight and obesity. Regarding diastolic function, the E/A ratio was lower along the increasing weight groups, whereas the E/e' average ratio showed higher values with each weight group. Regarding STE-derived indices, LVGLS showed a progressive decline across the three weight groups, with normal-weight individuals having the highest absolute LVGLS values and subjects with obesity having the lowest. Concerning MW indices, GWI and GCW values were significantly lower in the obese group, while there was no difference between the normal-weight and overweight groups. Conversely, GWW and GWE values were comparable between the weight groups (Table 7). Furthermore, we have compared patients with and without outcomes within the three weight groups (70).

Table 7. Echocardiographic parameters of study population according to body mass index category

	Overall (n=1330)	Normal weight (n=405)	Overweight (n=526)	Obese (n=399)	p-value
2D conventional echocardiographic data					
LVIDd, mm	48.29±4.79	46.02±4.07[bc]	48.68±4.50[ac]	50.17±4.93[ab]	**<0.001**
IVSd, mm	9.94±1.75	9.10±1.50[bc]	10.09±1.68[ac]	10.62±1.74[ab]	**<0.001**
PWd, mm	9.37±1.51	8.57±1.36[bc]	9.58±1.43[ac]	9.92±1.42[ab]	**<0.001**
RWT, %	0.44±0.13	0.41±0.12[bc]	0.46±0.14[a]	0.45±0.14[a]	**<0.001**
LVMi, g/m^2	87.50±21.52	79.20±18.43[bc]	89.79±21.74[a]	93.14±21.71[a]	**<0.001**
LV ESVi, ml/m^2	20.63±4.98	20.30±5.11	21.06±5.09	20.41±4.68	**0.041**
LV EDVi, ml/m^2	59.15±11.09	57.00±10.65[bc]	60.62±11.39[a]	59.40±10.81[a]	**<0.001**
EF, %	65.11±5.21	64.44±5.14[bc]	65.29±5.08[a]	65.54±5.41[a]	**0.007**
E, cm/s	76.40±17.69	80.80±17.32[bc]	73.55±16.22[a]	75.76±19.02[a]	**<0.001**
A, cm/s	68.88±21.00	61.00±19.52[bc]	67.88±19.87[ac]	77.93±20.45[ab]	**<0.001**
E/A	1.22±0.51	1.47±0.60[bc]	1.18±0.47[ac]	1.03±0.36[ab]	**<0.001**
DT (ms)	201.89±58.58	188.52±56.87[bc]	205.01±57.32[a]	210.93±59.68[a]	**<0.001**
Mitral lateral s', cm/s	9.88±2.69	10.60±2.73[bc]	9.66±2.62[a]	9.45±2.60[a]	**<0.001**
Mitral lateral e', cm/s	12.31±4.17	14.48±4.34[bc]	11.93±4.07[ac]	10.63±3.06[ab]	**<0.001**
Mitral lateral a', cm/s	10.39±3.18	9.36±2.99[bc]	10.58±3.08[ac]	11.17±3.21[ab]	**<0.001**
Mitral medial s', cm/s	8.58±1.79	8.80±1.84[c]	8.61±1.72[c]	8.31±1.79[ab]	**<0.001**
Mitral medial e', cm/s	9.80±3.38	11.65±3.62[bc]	9.46±3.11[ac]	8.36±2.53[ab]	**<0.001**

Mitral medial a', cm/s	10.46±2.42	9.75±2.66^{bc}	10.88±2.27^{a}	10.64±2.17^{a}	**<0.001**
E/e' average	7.47±2.59	6.64±2.44^{bc}	7.39±2.39^{ac}	8.38±2.70^{ab}	**<0.001**
LAVi, ml/m^2	28.94±9.88	26.67±9.21^{bc}	29.35±9.58^{a}	30.70±10.49^{a}	**<0.001**
RVd, mm	34.62±5.41	33.20±4.61^{bc}	35.06±5.72^{a}	35.50±5.47^{a}	**<0.001**
RAVi, ml/m^2	23.13±7.88	23.15±7.94	23.65±7.99	22.40±7.62	0.069
TAPSE, mm	23.85±4.04	24.00±4.07	23.99±3.89	23.51±4.17	0.149
Speckle tracking echocardiography data					
LV GLS, %	-19.94±3.49	-20.86±3.55^{bc}	-19.95±3.33^{ac}	-18.99±3.39^{ab}	**<0.001**
Myocardial work data					
GWI, mmHg %	2040.65±483.64	2062.04±489.65^{c}	2076.51±468.3^{c}	1971.66±491.4^{ab}	**0.003**
GCW, mmHg %	2194.21±472.40	2227.67±466.36^{c}	2236.33±463.3^{c}	2104.74±479.3^{ab}	**<0.001**
GWW, mmHg %	144.97±104.14	146.78±106.50	147.37±104.63	139.97±101.11	0.517
GWE, %	93.72±4.27	93.75±4.29	93.73±4.22	93.66±4.31	0.952

Continuous variables are presented as means ± SD. a: $p < 0.05$ vs. Normal weight, b: $p < 0.05$ vs. Overweight, c: $p < 0.05$ vs. Obese. A, atrial contraction; a', peak late (atrial) diastolic annular velocity; DT, deceleration time; E, early diastolic filling; e', early diastolic annular velocity; EDVi, end diastolic volume index; EF, ejection fraction; ESVi, end-systolic volume index; GCW, global constructive work; GLS, global longitudinal strain; GWE, global work efficiency; GWI, global work index; GWW, global wasted work; IVSd, inter-ventricular septal diameter; LAVi, left atrial volume index; LV, left ventricle; LVIDd, left ventricular internal diameter at end-diastole; LVMi, left ventricular mass index; PWd, posterior wall diameter; RAVi, right atrial volume index; RVd, right ventricle diameter; RWT, relative wall thickness; s', systolic annular velocity; TAPSE, tricuspid annular plane systolic excursion.

4.2.5 Long-term prognostic value of LV systolic function in different weight groups

We have performed univariable Cox regression analysis in the total cohort and within the 3 different weight groups (Table 8). Focusing on the prognostic value of LV systolic function; in the total cohort, LVEF was not associated with the adverse outcome, whereas LVGLS, GWI, GWE, and GWW were significant predictors of all-cause mortality (Table 8). Conversely, when assessing the normal weight group only LVGLS was a predictor of the adverse outcome, whereas LVEF or MW metrics were not (Table 8). In the overweight group, LVGLS, along with GWE and GWW, were significant predictors, whereas LVEF, GWI, and GCW were not (Table 8). Finally, in the obese group, only GWI emerged as a significant predictor of all-cause mortality (Table 8) (70). To adjust for potential clinical cofounders, multivariable Cox regression models were built based on clinical differences observed in Table 6. When adjusting for female sex, BMI, and systolic blood pressure, GWI still remained an independent significant predictor of all-cause mortality in the total cohort, and in patients with overweight and obesity, but interestingly not in patients with normal weight (Table 8) (70).

Furthermore, participants were dichotomized based on a previously established GWI cut-off value of 1292 mmHg% (70). Applying this threshold, GWI effectively differentiated between high-risk and low-risk groups in terms of all-cause mortality in the total cohort, and in the overweight and obese subgroups, but not in the normal weight group (Figure 7). As the Kaplan–Meier survival curves indicate, those overweight subjects with GWI values below 1292 mmHg% experienced more than 3-fold increase in the risk of all-cause mortality (Figure 7C). Similarly, in the obese subgroup (Figure 7D) and in the total cohort (Figure 7A), participants with GWI values below the cut-off had more than 2-times increased risk for adverse events (70). Moreover, multivariable Cox proportional hazard models were also built adjusting for the previously used confounders (female sex SBP, BMI). Even after adjusting for relevant clinical variables, the guideline-based GWI cutoff was independently associated with the outcome, as patients with GWI values below 1292 mmHg% experienced a higher risk of all-cause mortality in the total cohort and in all weight groups respectively (70).

Table 8. Association of echocardiography-derived LV systolic function metrics with all-cause mortality in different weight groups using univariable and multivariable Cox regression

	Total Cohort (n=1330)		Normal weight (n=405)		Overweight (n=526)		Obesity (n=399)	
Univariable Cox regressions in different subgroups								
	HR [95% CI]	**p-value**	**HR [95% CI]**	**p-value**	**HR [95% CI]**	**p-value**	**HR [95% CI]**	**p-value**
LVEF	0.971 [0.941-1.002]	0.066	0.966 [0.892-1.045]	0.385	0.961 [0.918-1.007]	0.093	0.972 [0.924-1.021]	0.259
LVGLS	1.100 [1.049-1.154]	**<0.001**	1.156 [1.031-1.295]	**0.013**	1.089 [1.014-1.170]	**0.020**	1.051 [0.967-1.141]	0.239
GWE	0.947 [0.914-0.981]	**0.002**	1.012 [0.915-1.119]	0.823	0.917 [0.874-0.963]	**<0.001**	0.964 [0.906-1.025]	0.238
GWI	0.958 [0.924-0.992]	**0.017**	1.001 [0.919-1.090]	0.984	0.976 [0.917-1.019]	0.212	0.929 [0.875-0.986]	**0.015**
GCW	0.979 [0.944-1.015]	0.243	1.002 [0.916-1.096]	0.970	1.003 [0.952-1.058]	0.902	0.943 [0.887-1.003]	0.064
GWW	1.194 [1.041-1.369]	**0.011**	0.938 [0.618-1.424]	0.764	1.341 [1.121-1.604]	**0.001**	1.109 [0.836-1.425]	0.419
Multivariable Cox regressions in different subgroups								
Female sex	0.517 [0.367-0.728]	**<0.001**	0.224 [0.091-0.553]	**0.001**	0.679 [0.411-1.120]	0.129	0.600 [0.335-1.075]	0.086
SBP	1.029 [1.019-1.038]	**<0.001**	1.049 [1.030-1.067]	**<0.001**	1.028 [1.014-1.041]	**<0.001**	1.012 [0.993-1.032]	0.209
BMI	1.016 [0.981-1.053]	0.365	0.832 [0.678-1.022]	0.080	0.938 [0.783-1.122]	0.482	1.027 [0.946-1.116]	0.526
GWI	**0.923 [0.889-0.959]**	**<0.001**	0.934 [0.856-1.019]	0.122	**0.922 [0.872-0.975]**	**0.005**	**0.920 [0.863-0.981]**	**0.011**

BMI, body mass index; CI, confidence interval; LVEF, left ventricular ejection fraction; GCW, global constructive work; GWE, global work efficiency; GWI, global work index; GWW, global wasted work; HR, hazard ratio; LVGLS, left ventricular global longitudinal strain; SBP, systolic blood pressure.

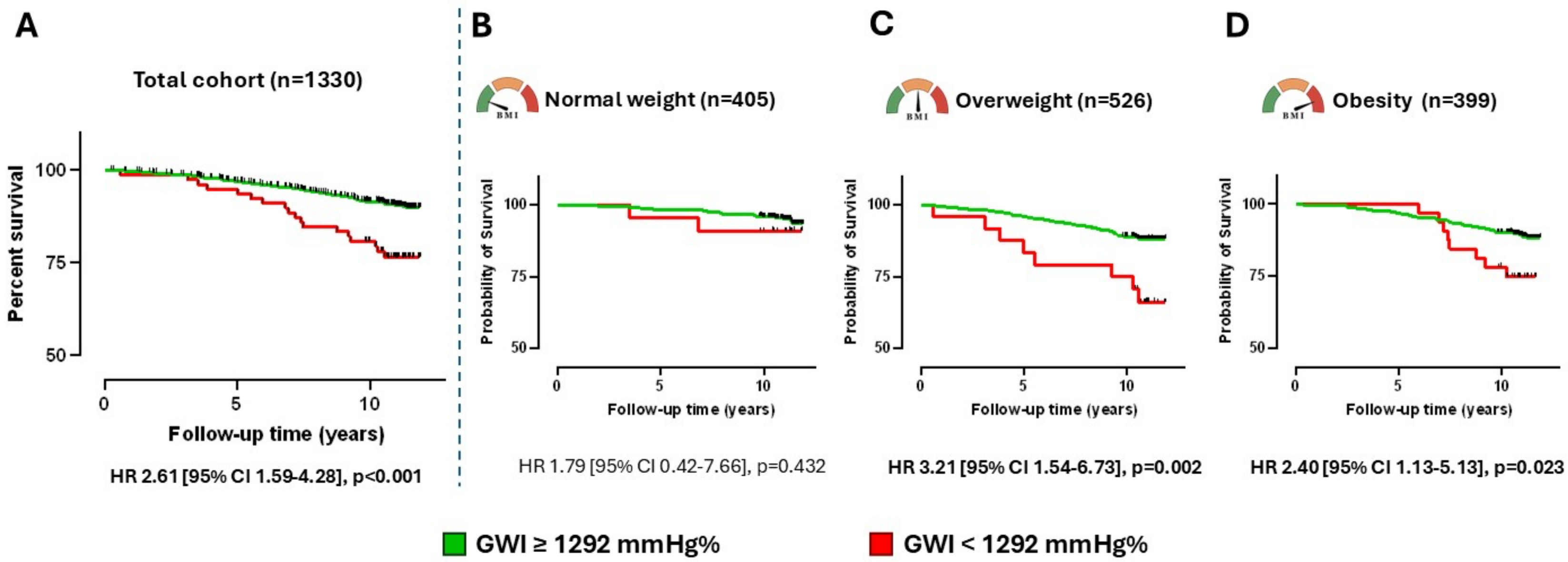

Figure 7. *Kaplan–Meier survival curves using the previously published cut-off value of 1292 mmHg% in total cohort (A), normal weight (B), overweight (C) and obese (D) groups. CI, confidence interval; GWI, global myocardial work index; HR, hazard ratio (70).*

5 Discussion

5.2 Investigation of the long-term prognostic importance of peak atrial longitudinal strain in a community-based screening sample comprising elderly individuals

With the growing clinical emphasis on HF with preserved LVEF (HFpEF), clinical and research efforts have increasingly shifted back to the assessment of diastolic dysfunction. In this context, beyond the conventional echocardiographic parameters of diastolic function, the evaluation of LA mechanics is of particular interest. Recently, novel techniques enabled the automated and accurate measurement of all three LA phasic functions, i.e., the reservoir, the conduit, and the contraction. Among these, reservoir strain (PALS) by 2D STE has emerged as a particularly robust parameter and, accordingly, served as the primary focus of our study, aiming to support the integration of LA mechanical assessment into routine screening protocols among the elderly, whose echocardiographic evaluation and risk stratification is a challenge in routine clinical practice.

As known, LV diastolic function exhibits deterioration with age (42, 71), however, there is evidence that LV diastolic dysfunction and increased LA volumes are independent predictors of first age-related cardiovascular event in an elderly population (30). Cacciapuoti et al. also confirmed the connection between LA function and volumes and age-related LV dysfunction (42). Regarding conventional echocardiographic parameters of the LA, numerous studies demonstrated their incremental diagnostic and prognostic value in different clinical scenarios. In routine clinical practice, the most commonly used parameter to assess left atrial structure is LAVi. In a study, with over 3.5 years of follow-up of 317 patients enrolled in sinus rhythm, LAVi outperformed LA area and M-mode LA dimensions in predicting the composite endpoint of the first occurrence of atrial fibrillation (AF), congestive HF, stroke, transient ischemic attack, acute myocardial infarction (AMI), coronary revascularization, and cardiovascular mortality. In addition, LAVi showed a graded association with overall event-free survival (72). Furthermore, a recent study by Inciardi et al. involving 4901 elderly participants confirmed that regardless of measures of LV function and NT-proBNP, higher minimal LAVi values, but not maximal LAVi values, along with novel indices of LA function were associated with a greater risk of incident HF and death (30).

Nevertheless, LA dysfunction may be even present despite a normal-size LA, and LAVi has demonstrated low sensitivity in the early detection of LV diastolic dysfunction (73). In contrast, 2D STE, is a readily available, semi-automated, and reproducible method that enables direct measurements of LA mechanics. Recently, several investigations have consistently shown that PALS is a reliable marker of LA reservoir function and correlates closely to LV filling pressures (74, 75). In HFpEF, a recent study suggested that PALS offers important clinical and prognostic value, underscoring the significant role of the LA in the pathophysiology of the disease course. PALS has been consistently associated with the severity of diastolic dysfunction (56). Of note, Morris et al. found that adding PALS to LAVi increased the detection rate of LV diastolic dysfunction. Considering clinical significance, even when LAVi remained in a normal range, the deterioration of PALS was strongly associated with worsening New York Heart Association functional class (73).

In the context of cardiovascular risk assessment in the general population, some recent studies have demonstrated the predictive utility of other STE-derived parameters such as LVGLS (31, 32). In a large community-based cohort, lower values of LVGLS were associated with future cardiovascular events independent of conventional risk factors. Furthermore, authors noted that the risk for cardiovascular events increased with the increasing number of LV abnormalities, such as impaired LV GLS, diastolic dysfunction, and LV hypertrophy (32). In a separate investigation analysing 1296 low-risk subjects, LVGLS provided incremental prognostic value beyond the Framingham risk score, the SCORE risk chart, and the modified ACC/ AHA Pooled Cohort Equation for predicting composite outcomes and incident HF. Notably, GLS was an independent predictor of outcomes in men but not in women (31). In our cohort, GLS was also impaired in individuals with adverse outcomes despite having similar LVEF. However, by multivariable analysis, PALS emerged as an independent predictor of outcome beyond the Framingham risk score. Accordingly, we hypothesize that the deterioration of LA function (diastolic dysfunction) may precede the development of LV systolic dysfunction; therefore, the assessment of LA mechanics may allow an earlier detection of cardiac abnormalities and improving prognostic accuracy for future adverse events. In a similar previous study, conducted by Modin et al. (76), the authors investigated the prognostic value of PALS in the general population and found that PALS emerged as a univariable predictor of adverse outcomes. However, its prognostic value was dependent on sex, as it was not a significant predictor in males (76). Another prospective study assessed the role of PALS in predicting cardiovascular outcomes in a cohort of 312 adults (77) and concluded that PALS was a strong and independent predictor of cardiovascular adverse events, appearing to be superior to other conventional echocardiographic markers of the LA**.** Similarly, Cameli et al. performed ROC analysis, and among all LA parameters, PALS exhibited the highest discriminatory power to identify patients-at-risk in an older, non-low-risk population. However, the study did not investigate whether the prognostic value of PALS was independent of LV function and was also limited by its relatively short follow-up (3.1 years) (77). In comparison to the above-mentioned studies, our findings add an important layer of clinical relevance by demonstrating that PALS is a significant predictor of long-term adverse outcomes independent of other "classical" cardiovascular risk estimators such as LV function, IMT, and the Agatston and Framingham scores. Our findings support the notion that measuring PALS by STE could enhance risk stratification in the general population in a convenient and cost-effective manner. This may also facilitate the early detection of those at risk for future adverse outcomes and the identification of the best candidates for long-term preventive measures. Importantly, our results do not diminish, but rather reinforce the value of the other imaging biomarkers assessed within the framework of this project. Both the Agatston score and IMT remain established cumulative markers of cardiovascular damage, with well-established prognostic value even in asymptomatic patients or in the context of non-cardiac diseases (78).

5.2 Evaluating the impact of overweight and obesity on myocardial work measures and assessing their prognostic power in a low-risk, community-based cohort

Given the rising global burden of obesity and its well-documented impact on cardiovascular health, clinical and research initiatives have increasingly focused on risk stratification of individuals with obesity. Echocardiography, as a cost-effective, non-invasive, and reliable diagnostic modality, offers added value in routine cardiovascular risk assessment for overweight and obese populations. Evaluating cardiac function is particularly important, as obesity is closely associated with structural, functional, and hemodynamic alterations that contribute to the development of cardiovascular diseases (79-81). It is also well recognized that in individuals with overweight or obesity, increased blood volume, elevated cardiac output, and systemic vascular resistance, along with the activation of the renin-angiotensin-aldosterone system and enhanced sympathetic activity, altogether lead to adverse cardiac remodelling and progressively deteriorating cardiac function (81, 82).

Several studies have demonstrated that obesity is associated with LV dilation, increased LV volumes, elevated mass index, and increased relative wall thickness (28, 83). In line with our findings, Chinali et al. also reported that obesity was linked not only to LV geometric abnormalities but also to reduced LVEF (83). Although LVEF remains a standard marker for evaluating systolic function in individuals with obesity, recently, more advanced techniques, such as STE-derived LVGLS, have received growing attention for detecting subclinical systolic dysfunction, particularly when LVEF remains within the normal range (29, 35, 36). Notably, a multicentre, cross-sectional study by Snelder et al. revealed a high prevalence of subclinical myocardial dysfunction among obese individuals without overt cardiovascular disease (29) which was most reliably detected by LVGLS and was linked to autonomic dysregulation rather than to traditional cardiovascular risk factors (29). These findings were also verified in our study, involving a large low-risk community-based cohort, as LVEF remained in normal ranges throughout all weight subgroups, whereas LVGLS showed a gradual decline with increasing BMI. However, despite the progressive deterioration in LVGLS, its prognostic role was limited in individuals with obesity. The prognostic value of GWI in individuals with obesity, particularly when conventional systolic markers such as LVEF and LVGLS remain maintained, suggests that MW analysis may serve as an additional tool in clinical risk assessment. Rather than offering a replacement for standard measures, it may complement them by unmasking early or subtle dysfunction in patients with underlying cardiometabolic processes who otherwise would be classified as low risk.

In our cohort, overweight individuals exhibited comparable GWI and GCW values to their normal-weight counterparts, despite the gradual decline of LVGLS values in the overweight group. This inconsistency likely reflects the hemodynamic and neurohormonal changes associated with increased BMI, including augmented preload and afterload, heightened sympathetic activation, all of which promote elevated blood pressure along with increased LV contractility and work. Indeed, our findings demonstrated that individuals with overweight had higher systolic and diastolic blood pressures than subjects in the normal-weight group, however, MW indices were comparable, likely attributable to the fact that MW analysis takes afterload into account. This, however, may not necessarily be interpreted as indicative of healthy cardiac function. In contrast, individuals with obesity demonstrated lower GWI and GCW compared to both overweight and normal weight groups, consistent with adverse LV remodelling and myocardial fibrosis associated with obesity stage. Notably, our findings are in line with previous studies reporting similar patterns of MW changes, marked by reductions in GCW and GWI, independent of systolic blood pressure (84, 85). While in early stages of obesity, elevated preload, afterload, and sympathetic activation result in maintained or even increased LV work and contractility, over time, these adaptive mechanisms may fail, leading to maladaptive changes such as fibrosis, inflammation, and metabolic dysfunction, adverse LV remodelling, ultimately resulting in reduced GWI.

In the context of cardiovascular risk assessment within a low-risk population, STE-derived parameters such as LVGLS and PALS have shown significant predictive value (31-33). However, evidence remains scarce regarding the long-term prognostic value of STE-derived systolic function metrics in obese and overweight individuals. Of note, our study demonstrated that LVGLS was a significant predictor of all-cause mortality in normal-weight and overweight individuals, but not among participants with obesity. Furthermore, when assessing the overweight group, both GWW and GWE were significant predictors of the outcome. These findings may reflect early metabolic dysregulation, including enhanced oxidative stress and inflammation in the myocardial tissue, resulting in ineffective contraction, thus impairing contractile efficiency and increasing wasted myocardial work. Additionally, elevated LV mass index, commonly observed in overweight individuals, may further contribute to the increased GWW, aligning with previous reports (83-85). Interestingly, in the group with obesity, GWI emerged as the only systolic function metric that predicted all-cause mortality, which may be partially attributed to the distinct hemodynamic changes associated with obesity, potentially hindering the interpretation of conventional markers such as GLS. Obesity is markedly characterized by an expanded volumetric state and increased venous return, leading to elevated preload, while concurrent arterial stiffening and increased systemic vascular resistance may contribute to a chronically increased afterload (86). Given this altered hemodynamic state, with opposing forces and the known load-dependency of strain metrics, GLS may lack sensitivity in detecting subclinical changes, thereby attenuating its prognostic value in patients with obesity. In contrast, GWI integrates information from two distinct domains: myocardial deformation and systemic load, capturing the cumulative effect associated with myocardial impairment (e.g., interstitial fibrosis, concentric remodelling) and hemodynamic burden (e.g., stiffening, altered ventricular-arterial coupling) arising from obesity. Therefore, MW metrics may better portray the interplay between altered myocardial mechanics and systemic load, serving as an integrative marker of increased cumulative risk associated with obesity.

Although recent studies, such as the work by Olsen et al., have investigated the prognostic value of MW indices in the general population, none have specifically addressed their role in association with obesity and within low-risk cohorts (87). The study by Olsen and colleagues demonstrated that GWI, GCW, and GWE were all associated with adverse outcomes in individuals with hypertension but did not explore the impact of obesity or overweight (87). Therefore, our results add an important dimension to the existing literature by highlighting the clinical relevance and importance of MW assessment in overweight and obese populations.

Importantly, while our results support the growing evidence of the prognostic utility of MW, their clinical application and integration into routine echocardiographic evaluation warrant further consideration. From a practical standpoint, GWI is derived from two domains already routinely acquired in standard echocardiographic protocols: STE-derived GLS quantification and non-invasive brachial blood pressure measurement. Moreover, MW analysis can be directly performed in real-time on most modern echocardiographic platforms using integrated, semi-automated software, and without requiring additional imaging, time burden, or extensive post-processing. Still, it is important to emphasize that, rather than serving as a standalone screening tool, MW analysis could complement conventional metrics such as LVEF and LVGLS by detecting subclinical deterioration and may reveal the cumulative burden of hemodynamic inefficiency or reduced contractile reserve in individuals with elevated cardiometabolic risk. When interpreted alongside demographic variables, clinical risk factors, and routine 2D echocardiographic metrics, MW may enhance individualized risk stratification and help guide closer follow-up, preventive strategies, or early interventions, particularly in patients with overweight and obesity.

5.2 Limitations

There are several limitations that should be recognized concerning the studies discussed above. These are retrospective, single-centre studies, which may affect the generalizability and interpretation of the findings. In the first study, strain analysis was performed by tracing the LA endocardium in only one imaging plane (apical four-chamber view). However, recent guidelines accept calculating PALS obtained from a single apical four-chamber view (50). In addition, while PALS was associated with all-cause mortality, the lack of cause-specific mortality data limits our ability to determine its predictive value specifically for cardiovascular-related outcomes. Additional studies, in larger cohorts with specified outcomes and adequate event rates, are needed to confirm our results. Using ROC analysis, PALS showed modest sensitivity and specificity, suggesting that while it may contribute to risk assessment, its use as a standalone screening tool may be limited.

However, its potential clinical utility lies in complementing conventional echocardiographic protocols, thereby enhancing clinical decision-making. From a clinical standpoint, these findings suggest that PALS is most valuable as an adjunct to refine risk stratification in subpopulations—such as the elderly or those with subclinical cardiovascular disease—where conventional scores may be insufficient. Rather than serving as a universal screening tool, integrating PALS into multimodal risk assessment frameworks could improve the detection of high-risk individuals and support targeted preventive strategies. Similarly, in our second study, we utilized only apical-four chamber views for the quantification of LV systolic function; however, this approach has been approved and validated in several previous studies (88, 89). While our study was the first to demonstrate the prognostic power of MW metrics in individuals with overweight and obesity in the general population, further prospective and multi-centre studies are required to validate and strengthen these results.

It is important to note that deformation imaging and myocardial work analysis remain underutilized in routine clinical practice, limiting the immediate application of these findings. However, the development of next-generation automated tools, which enable rapid and reproducible measurement of MW metrics and PALS, could facilitate broader adoption and clinical implementation of these valuable metrics.

6 Conclusion

In our first study, we were able to determine the long-term prognostic importance of STE-derived peak atrial longitudinal strain (PALS) in a community-based screening sample comprising elderly individuals. PALS offered incremental value in cardiovascular risk stratification in a community-based cohort, beyond the assessment of LV systolic functional parameters such as LVEF and LVGLS. By multivariable regression models, PALS was found to be a significant and independent predictor of long-term all-cause mortality. These results emphasize the importance of a thorough evaluation of LA mechanics in an elderly population.

Regarding the second study, we assessed the impact of overweight and obesity on myocardial work measures and investigated their prognostic power in a low-risk, community-based cohort. Myocardial work analysis-derived metrics were found to be robust and independent predictors of all-cause mortality in low-risk individuals with different stages of obesity. These findings underscore the limitations of conventional echocardiographic measures, which may underestimate cardiovascular risk in overweight and obese populations, highlighting the potential of MW analysis to refine risk stratification and improve prognostic accuracy in this growing patient cohort.

7 Summary

Accurate cardiovascular risk assessment is pivotal in preventive cardiology, as it enables early identification of individuals at elevated risk of CVD. While traditional risk prediction models have proven useful, they bear notable limitations, particularly in stratifying risk among low-risk individuals and those with subclinical diseases.

Obesity remains a well-established risk factor for CVD, yet assessing cardiovascular risk in individuals with obesity is particularly challenging. These insights have spurred interest in more advanced diagnostic tools that enable the unmasking of early cardiovascular dysfunction in this population. Risk prediction is similarly complex in the elderly, where physiological aging and the cumulative burden of comorbidities undermine the accuracy of traditional scoring systems.

Echocardiography has become a cornerstone in cardiovascular diagnostics. While traditional markers such as LVEF remain the standard for systolic function, novel approaches such as STE-derived GLS and MW analysis offer improved sensitivity to detect subclinical cardiac dysfunction. In addition to systolic function, STE-based assessment of LA mechanics has gained attention as an early indicator of diastolic dysfunction.

Our studies have demonstrated that PALS is a strong and independent predictor of long-term outcomes in older adults, beyond traditional markers such as LVGLS, carotid intima-media thickness, coronary calcium score, and the Framingham risk score.

Furthermore, GWI was shown to be a robust predictor of all-cause mortality in low-risk individuals across different stages of obesity, reinforcing the value of MW in detecting early myocardial dysfunction and improving long-term prognostic risk assessment.

In conclusion, our findings support the clinical utility of advanced echocardiographic techniques, including STE-derived left atrial longitudinal strain and myocardial work indices as valuable tools to improve cardiovascular risk assessment, especially in populations where conventional models are limited, such as the elderly and individuals with obesity.

8 References

1. German CA, Baum SJ, Ferdinand KC, Gulati M, Polonsky TS, Toth PP, Shapiro MD. Defining preventive cardiology: A clinical practice statement from the American Society for Preventive Cardiology. Am J Prev Cardiol. 2022;12:100432.

2. WHO. Cardiovascular Diseases Fact Sheet 2025 [Available from: https://www.who.int/news-room/fact-sheets/detail/cardiovascular-diseases-(cvds).

3. WHO. Global action plan for the prevention and control of noncommunicable diseases 2013-2020 [Available from: https://www.who.int/publications/i/item/9789241506236.

4. Yusuf S, Hawken S, Ounpuu S, Dans T, Avezum A, Lanas F, McQueen M, Budaj A, Pais P, Varigos J, Lisheng L. Effect of potentially modifiable risk factors associated with myocardial infarction in 52 countries (the INTERHEART study): case-control study. Lancet. 2004;364(9438):937–52.

5. Roth GA, Mensah GA, Johnson CO, Addolorato G, Ammirati E, Baddour LM, Barengo NC, Beaton AZ, Benjamin EJ, Benziger CP, Bonny A, Brauer M, Brodmann M, Cahill TJ, Carapetis J, Catapano AL, Chugh SS, Cooper LT, Coresh J, Criqui M, DeCleene N, Eagle KA, Emmons-Bell S, Feigin VL, Fernández-Solà J, Fowkes G, Gakidou E, Grundy SM, He FJ, Howard G, Hu F, Inker L, Karthikeyan G, Kassebaum N, Koroshetz W, Lavie C, Lloyd-Jones D, Lu HS, Mirijello A, Temesgen AM, Mokdad A, Moran AE, Muntner P, Narula J, Neal B, Ntsekhe M, Moraes de Oliveira G, Otto C, Owolabi M, Pratt M, Rajagopalan S, Reitsma M, Ribeiro ALP, Rigotti N, Rodgers A, Sable C, Shakil S, Sliwa-Hahnle K, Stark B, Sundström J, Timpel P, Tleyjeh IM, Valgimigli M, Vos T, Whelton PK, Yacoub M, Zuhlke L, Murray C, Fuster V. Global Burden of Cardiovascular Diseases and Risk Factors, 1990-2019: Update From the GBD 2019 Study. J Am Coll Cardiol. 2020;76(25):2982–3021.

6. Benjamin EJ, Muntner P, Alonso A, Bittencourt MS, Callaway CW, Carson AP, Chamberlain AM, Chang AR, Cheng S, Das SR, Delling FN, Djousse L, Elkind MSV, Ferguson JF, Fornage M, Jordan LC, Khan SS, Kissela BM, Knutson KL, Kwan TW, Lackland DT, Lewis TT, Lichtman JH, Longenecker CT, Loop MS, Lutsey PL, Martin SS,

Matsushita K, Moran AE, Mussolino ME, O'Flaherty M, Pandey A, Perak AM, Rosamond WD, Roth GA, Sampson UKA, Satou GM, Schroeder EB, Shah SH, Spartano NL, Stokes A, Tirschwell DL, Tsao CW, Turakhia MP, VanWagner LB, Wilkins JT, Wong SS, Virani SS. Heart Disease and Stroke Statistics-2019 Update: A Report From the American Heart Association. Circulation. 2019;139(10):e56–e528.

7. Visseren FLJ, Mach F, Smulders YM, Carballo D, Koskinas KC, Bäck M, Benetos A, Biffi A, Boavida JM, Capodanno D, Cosyns B, Crawford C, Davos CH, Desormais I, Di Angelantonio E, Franco OH, Halvorsen S, Hobbs FDR, Hollander M, Jankowska EA, Michal M, Sacco S, Sattar N, Tokgozoglu L, Tonstad S, Tsioufis KP, van Dis I, van Gelder IC, Wanner C, Williams B. 2021 ESC Guidelines on cardiovascular disease prevention in clinical practice. Eur Heart J. 2021;42(34):3227–337.

8. Barton P, Andronis L, Briggs A, McPherson K, Capewell S. Effectiveness and cost effectiveness of cardiovascular disease prevention in whole populations: modelling study. Bmj. 2011;343:d4044.

9. SCORE2 risk prediction algorithms: new models to estimate 10-year risk of cardiovascular disease in Europe. Eur Heart J. 2021;42(25):2439–54.

10. Goff DC, Jr., Lloyd-Jones DM, Bennett G, Coady S, D'Agostino RB, Gibbons R, Greenland P, Lackland DT, Levy D, O'Donnell CJ, Robinson JG, Schwartz JS, Shero ST, Smith SC, Jr., Sorlie P, Stone NJ, Wilson PW, Jordan HS, Nevo L, Wnek J, Anderson JL, Halperin JL, Albert NM, Bozkurt B, Brindis RG, Curtis LH, DeMets D, Hochman JS, Kovacs RJ, Ohman EM, Pressler SJ, Sellke FW, Shen WK, Tomaselli GF. 2013 ACC/AHA guideline on the assessment of cardiovascular risk: a report of the American College of Cardiology/American Heart Association Task Force on Practice Guidelines. Circulation. 2014;129(25 Suppl 2):S49–73.

11. Wilson PW, D'Agostino RB, Levy D, Belanger AM, Silbershatz H, Kannel WB. Prediction of coronary heart disease using risk factor categories. Circulation. 1998;97(18):1837–47.

12. collaboration S-OwgaECr. SCORE2-OP risk prediction algorithms: estimating incident cardiovascular event risk in older persons in four geographical risk regions. Eur Heart J. 2021;42(25):2455–67.

13. Piepoli MF, Hoes AW, Agewall S, Albus C, Brotons C, Catapano AL, Cooney MT, Corrà U, Cosyns B, Deaton C, Graham I, Hall MS, Hobbs FDR, Løchen ML, Löllgen H, Marques-Vidal P, Perk J, Prescott E, Redon J, Richter DJ, Sattar N, Smulders Y, Tiberi M, van der Worp HB, van Dis I, Verschuren WMM, Binno S. 2016 European Guidelines on cardiovascular disease prevention in clinical practice: The Sixth Joint Task Force of the European Society of Cardiology and Other Societies on Cardiovascular Disease Prevention in Clinical Practice (constituted by representatives of 10 societies and by invited experts)Developed with the special contribution of the European Association for Cardiovascular Prevention & Rehabilitation (EACPR). Eur Heart J. 2016;37(29):2315–81.

14. Arnett DK, Blumenthal RS, Albert MA, Buroker AB, Goldberger ZD, Hahn EJ, Himmelfarb CD, Khera A, Lloyd-Jones D, McEvoy JW, Michos ED, Miedema MD, Muñoz D, Smith SC, Jr., Virani SS, Williams KA, Sr., Yeboah J, Ziaeian B. 2019 ACC/AHA Guideline on the Primary Prevention of Cardiovascular Disease: A Report of the American College of Cardiology/American Heart Association Task Force on Clinical Practice Guidelines. Circulation. 2019;140(11):e596–e646.

15. Lakatta EG, Levy D. Arterial and cardiac aging: major shareholders in cardiovascular disease enterprises: Part II: the aging heart in health: links to heart disease. Circulation. 2003;107(2):346–54.

16. Lakatta EG, Levy D. Arterial and cardiac aging: major shareholders in cardiovascular disease enterprises: Part I: aging arteries: a "set up" for vascular disease. Circulation. 2003;107(1):139–46.

17. Lind L, Sundström J, Ärnlöv J, Lampa E. Impact of Aging on the Strength of Cardiovascular Risk Factors: A Longitudinal Study Over 40 Years. J Am Heart Assoc. 2018;7(1).

18. Dalton JE, Rothberg MB, Dawson NV, Krieger NI, Zidar DA, Perzynski AT. Failure of Traditional Risk Factors to Adequately Predict Cardiovascular Events in Older Populations. J Am Geriatr Soc. 2020;68(4):754–61.

19. Nasir K, Rubin J, Blaha MJ, Shaw LJ, Blankstein R, Rivera JJ, Khan AN, Berman D, Raggi P, Callister T, Rumberger JA, Min J, Jones SR, Blumenthal RS, Budoff MJ. Interplay

of coronary artery calcification and traditional risk factors for the prediction of all-cause mortality in asymptomatic individuals. Circ Cardiovasc Imaging. 2012;5(4):467–73.

20. WHO. 2024 [Available from: https://www.who.int/news-room/fact-sheets/detail/obesity-and-overweight.

21. Worldwide trends in body-mass index, underweight, overweight, and obesity from 1975 to 2016: a pooled analysis of 2416 population-based measurement studies in 128·9 million children, adolescents, and adults. Lancet. 2017;390(10113):2627–42.

22. Global BMIMC, Di Angelantonio E, Bhupathiraju Sh N, Wormser D, Gao P, Kaptoge S, Berrington de Gonzalez A, Cairns BJ, Huxley R, Jackson Ch L, Joshy G, Lewington S, Manson JE, Murphy N, Patel AV, Samet JM, Woodward M, Zheng W, Zhou M, Bansal N, Barricarte A, Carter B, Cerhan JR, Smith GD, Fang X, Franco OH, Green J, Halsey J, Hildebrand JS, Jung KJ, Korda RJ, McLerran DF, Moore SC, O'Keeffe LM, Paige E, Ramond A, Reeves GK, Rolland B, Sacerdote C, Sattar N, Sofianopoulou E, Stevens J, Thun M, Ueshima H, Yang L, Yun YD, Willeit P, Banks E, Beral V, Chen Z, Gapstur SM, Gunter MJ, Hartge P, Jee SH, Lam TH, Peto R, Potter JD, Willett WC, Thompson SG, Danesh J, Hu FB. Body-mass index and all-cause mortality: individual-participant-data meta-analysis of 239 prospective studies in four continents. Lancet. 2016;388(10046):776–86.

23. Koskinas KC, Van Craenenbroeck EM, Antoniades C, Blüher M, Gorter TM, Hanssen H, Marx N, McDonagh TA, Mingrone G, Rosengren A, Prescott EB. Obesity and cardiovascular disease: an ESC clinical consensus statement. Eur Heart J. 2024.

24. Lopez-Jimenez F, Almahmeed W, Bays H, Cuevas A, Di Angelantonio E, le Roux CW, Sattar N, Sun MC, Wittert G, Pinto FJ, Wilding JPH. Obesity and cardiovascular disease: mechanistic insights and management strategies. A joint position paper by the World Heart Federation and World Obesity Federation. Eur J Prev Cardiol. 2022;29(17):2218–37.

25. Caleyachetty R, Thomas GN, Toulis KA, Mohammed N, Gokhale KM, Balachandran K, Nirantharakumar K. Metabolically Healthy Obese and Incident Cardiovascular Disease Events Among 3.5 Million Men and Women. J Am Coll Cardiol. 2017;70(12):1429–37.

26. Ferrannini E, Natali A, Bell P, Cavallo-Perin P, Lalic N, Mingrone G. Insulin resistance and hypersecretion in obesity. European Group for the Study of Insulin Resistance (EGIR). J Clin Invest. 1997;100(5):1166–73.

27. Smith GI, Mittendorfer B, Klein S. Metabolically healthy obesity: facts and fantasies. J Clin Invest. 2019;129(10):3978–89.
28. Peterson LR, Waggoner AD, Schechtman KB, Meyer T, Gropler RJ, Barzilai B, Dávila-Román VG. Alterations in left ventricular structure and function in young healthy obese women: assessment by echocardiography and tissue Doppler imaging. J Am Coll Cardiol. 2004;43(8):1399–404.
29. Snelder SM, de Groot-de Laat LE, Biter LU, Castro Cabezas M, Pouw N, Birnie E, Boxma-de Klerk BM, Klaassen RA, Zijlstra F, van Dalen BM. Subclinical cardiac dysfunction in obesity patients is linked to autonomic dysfunction: findings from the CARDIOBESE study. ESC Heart Fail. 2020;7(6):3726–37.
30. Inciardi RM, Claggett B, Minamisawa M, Shin SH, Selvaraj S, Gonçalves A, Wang W, Kitzman D, Matsushita K, Prasad NG, Su J, Skali H, Shah AM, Chen LY, Solomon SD. Association of Left Atrial Structure and Function With Heart Failure in Older Adults. J Am Coll Cardiol. 2022;79(16):1549–61.
31. Biering-Sørensen T, Biering-Sørensen SR, Olsen FJ, Sengeløv M, Jørgensen PG, Mogelvang R, Shah AM, Jensen JS. Global Longitudinal Strain by Echocardiography Predicts Long-Term Risk of Cardiovascular Morbidity and Mortality in a Low-Risk General Population: The Copenhagen City Heart Study. Circ Cardiovasc Imaging. 2017;10(3).
32. Kuznetsova T, Cauwenberghs N, Knez J, Yang WY, Herbots L, D'Hooge J, Haddad F, Thijs L, Voigt JU, Staessen JA. Additive Prognostic Value of Left Ventricular Systolic Dysfunction in a Population-Based Cohort. Circ Cardiovasc Imaging. 2016;9(7).
33. Zhubi Bakija F, Bagyura Z, Fábián A, Ferencz A, Kiss L, Szenczi O, Vadas R, Dósa E, Nguyen DT, Csobay-Novák C, Jermendy Á L, Szelid Z, Soós P, Kovács A, Merkely B. Long-term prognostic value of left atrial longitudinal strain in an elderly community-based cohort. Geroscience. 2023;45(1):613–25.
34. Lang RM, Badano LP, Mor-Avi V, Afilalo J, Armstrong A, Ernande L, Flachskampf FA, Foster E, Goldstein SA, Kuznetsova T, Lancellotti P, Muraru D, Picard MH, Rietzschel ER, Rudski L, Spencer KT, Tsang W, Voigt JU. Recommendations for cardiac chamber quantification by echocardiography in adults: an update from the American Society of

Echocardiography and the European Association of Cardiovascular Imaging. J Am Soc Echocardiogr. 2015;28(1):1–39.e14.

35. Di Bello V, Fabiani I, Conte L, Barletta V, Delle Donne MG, Cuono C, Leo LA, Dini FL, Marzilli M, Pinchera A, Santini F. New echocardiographic techniques in the evaluation of left ventricular function in obesity. Obesity (Silver Spring). 2013;21(5):881–92.

36. Garg PK, Biggs ML, Kizer JR, Shah SJ, Djousse L, Mukamal KJ. Associations of body size and composition with subclinical cardiac dysfunction in older individuals: the cardiovascular health study. Int J Obes (Lond). 2021;45(12):2539–45.

37. Hubert A, Le Rolle V, Leclercq C, Galli E, Samset E, Casset C, Mabo P, Hernandez A, Donal E. Estimation of myocardial work from pressure-strain loops analysis: an experimental evaluation. Eur Heart J Cardiovasc Imaging. 2018;19(12):1372–9.

38. Russell K, Eriksen M, Aaberge L, Wilhelmsen N, Skulstad H, Remme EW, Haugaa KH, Opdahl A, Fjeld JG, Gjesdal O, Edvardsen T, Smiseth OA. A novel clinical method for quantification of regional left ventricular pressure-strain loop area: a non-invasive index of myocardial work. Eur Heart J. 2012;33(6):724–33.

39. SCORE2-OP risk prediction algorithms: estimating incident cardiovascular event risk in older persons in four geographical risk regions. Eur Heart J. 2021;42(25):2455–67.

40. Brecht A, Oertelt-Prigione S, Seeland U, Rücke M, Hättasch R, Wagelöhner T, Regitz-Zagrosek V, Baumann G, Knebel F, Stangl V. Left Atrial Function in Preclinical Diastolic Dysfunction: Two-Dimensional Speckle-Tracking Echocardiography-Derived Results from the BEFRI Trial. J Am Soc Echocardiogr. 2016;29(8):750–8.

41. Levene J, Voigt A, Thoma F, Mulukutla S, Bhonsale A, Kancharla K, Shalaby A, Estes NAM, 3rd, Jain S, Saba S. Patient Outcomes by Ventricular Systolic and Diastolic Function. J Am Heart Assoc. 2024;13(4):e033211.

42. Cacciapuoti F, Paoli VD, Scognamiglio A, Caturano M. Left Atrial Longitudinal Speckle Tracking Echocardiography in Healthy Aging Heart. J Cardiovasc Echogr. 2015;25(2):40–5.

43. Voigt JU, Pedrizzetti G, Lysyansky P, Marwick TH, Houle H, Baumann R, Pedri S, Ito Y, Abe Y, Metz S, Song JH, Hamilton J, Sengupta PP, Kolias TJ, d'Hooge J, Aurigemma GP, Thomas JD, Badano LP. Definitions for a common standard for 2D speckle tracking

echocardiography: consensus document of the EACVI/ASE/Industry Task Force to standardize deformation imaging. Eur Heart J Cardiovasc Imaging. 2015;16(1):1–11.

44. Voigt JU, Cvijic M. 2- and 3-Dimensional Myocardial Strain in Cardiac Health and Disease. JACC Cardiovasc Imaging. 2019;12(9):1849–63.

45. Blessberger H, Binder T. NON-invasive imaging: Two dimensional speckle tracking echocardiography: basic principles. Heart. 2010;96(9):716–22.

46. Hung CL, Verma A, Uno H, Shin SH, Bourgoun M, Hassanein AH, McMurray JJ, Velazquez EJ, Kober L, Pfeffer MA, Solomon SD. Longitudinal and circumferential strain rate, left ventricular remodeling, and prognosis after myocardial infarction. J Am Coll Cardiol. 2010;56(22):1812–22.

47. Mignot A, Donal E, Zaroui A, Reant P, Salem A, Hamon C, Monzy S, Roudaut R, Habib G, Lafitte S. Global longitudinal strain as a major predictor of cardiac events in patients with depressed left ventricular function: a multicenter study. J Am Soc Echocardiogr. 2010;23(10):1019–24.

48. Sengeløv M, Jørgensen PG, Jensen JS, Bruun NE, Olsen FJ, Fritz-Hansen T, Nochioka K, Biering-Sørensen T. Global Longitudinal Strain Is a Superior Predictor of All-Cause Mortality in Heart Failure With Reduced Ejection Fraction. JACC Cardiovasc Imaging. 2015;8(12):1351–9.

49. Shah AM, Claggett B, Sweitzer NK, Shah SJ, Anand IS, Liu L, Pitt B, Pfeffer MA, Solomon SD. Prognostic Importance of Impaired Systolic Function in Heart Failure With Preserved Ejection Fraction and the Impact of Spironolactone. Circulation. 2015;132(5):402–14.

50. Badano LP, Kolias TJ, Muraru D, Abraham TP, Aurigemma G, Edvardsen T, D'Hooge J, Donal E, Fraser AG, Marwick T, Mertens L, Popescu BA, Sengupta PP, Lancellotti P, Thomas JD, Voigt JU. Standardization of left atrial, right ventricular, and right atrial deformation imaging using two-dimensional speckle tracking echocardiography: a consensus document of the EACVI/ASE/Industry Task Force to standardize deformation imaging. Eur Heart J Cardiovasc Imaging. 2018;19(6):591–600.

51. Pathan F, D'Elia N, Nolan MT, Marwick TH, Negishi K. Normal Ranges of Left Atrial Strain by Speckle-Tracking Echocardiography: A Systematic Review and Meta-Analysis. J Am Soc Echocardiogr. 2017;30(1):59–70.e8.

52. Gan GCH, Ferkh A, Boyd A, Thomas L. Left atrial function: evaluation by strain analysis. Cardiovasc Diagn Ther. 2018;8(1):29–46.

53. Mada RO, Lysyansky P, Daraban AM, Duchenne J, Voigt JU. How to define end-diastole and end-systole?: Impact of timing on strain measurements. JACC Cardiovasc Imaging. 2015;8(2):148–57.

54. Singh A, Addetia K, Maffessanti F, Mor-Avi V, Lang RM. LA Strain for Categorization of LV Diastolic Dysfunction. JACC Cardiovasc Imaging. 2017;10(7):735–43.

55. Thomas L, Marwick TH, Popescu BA, Donal E, Badano LP. Left Atrial Structure and Function, and Left Ventricular Diastolic Dysfunction: JACC State-of-the-Art Review. J Am Coll Cardiol. 2019;73(15):1961–77.

56. Frydas A, Morris DA, Belyavskiy E, Radhakrishnan AK, Kropf M, Tadic M, Roessig L, Lam CSP, Shah SJ, Solomon SD, Pieske B, Pieske-Kraigher E. Left atrial strain as sensitive marker of left ventricular diastolic dysfunction in heart failure. ESC Heart Fail. 2020;7(4):1956–65.

57. Leung DY, Chi C, Allman C, Boyd A, Ng AC, Kadappu KK, Leung M, Thomas L. Prognostic implications of left atrial volume index in patients in sinus rhythm. Am J Cardiol. 2010;105(11):1635–9.

58. Obokata M, Negishi K, Kurosawa K, Tateno R, Tange S, Arai M, Amano M, Kurabayashi M. Left atrial strain provides incremental value for embolism risk stratification over CHA_2DS_2-VASc score and indicates prognostic impact in patients with atrial fibrillation. J Am Soc Echocardiogr. 2014;27(7):709–16.e4.

59. Sachdeva S, Desai R, Andi K, Vyas A, Deliwala S, Sachdeva R, Kumar G. Reduced left atrial strain can predict stroke in atrial fibrillation - A meta-analysis. Int J Cardiol Heart Vasc. 2021;36:100859.

60. Butcher SC, Lustosa RP, Abou R, Marsan NA, Bax JJ, Delgado V. Prognostic implications of left ventricular myocardial work index in patients with ST-segment elevation

myocardial infarction and reduced left ventricular ejection fraction. Eur Heart J Cardiovasc Imaging. 2022;23(5):699–707.

61. Hedwig F, Nemchyna O, Stein J, Knosalla C, Merke N, Knebel F, Hagendorff A, Schoenrath F, Falk V, Knierim J. Myocardial Work Assessment for the Prediction of Prognosis in Advanced Heart Failure. Front Cardiovasc Med. 2021;8:691611.

62. Moya A, Buytaert D, Penicka M, Bartunek J, Vanderheyden M. State-of-the-Art: Noninvasive Assessment of Left Ventricular Function Through Myocardial Work. J Am Soc Echocardiogr. 2023;36(10):1027–42.

63. Tokodi M, Oláh A, Fábián A, Lakatos BK, Hizoh I, Ruppert M, Sayour AA, Barta BA, Kiss O, Sydó N, Csulak E, Ladányi Z, Merkely B, Kovács A, Radovits T. Novel insights into the athlete's heart: is myocardial work the new champion of systolic function? Eur Heart J Cardiovasc Imaging. 2022;23(2):188–97.

64. Bagyura Z, Kiss L, Edes E, Lux A, Polgár L, Soós P, Szenczi O, Szelid Z, Vadas R, Józan P, Bagdy G, Merkely B. [Cardiovascular screening programme in the Central Hungarian region. The Budakalász Study]. Orv Hetil. 2014;155(34):1344–52.

65. D'Agostino RB, Sr., Vasan RS, Pencina MJ, Wolf PA, Cobain M, Massaro JM, Kannel WB. General cardiovascular risk profile for use in primary care: the Framingham Heart Study. Circulation. 2008;117(6):743–53.

66. Touboul PJ, Hennerici MG, Meairs S, Adams H, Amarenco P, Bornstein N, Csiba L, Desvarieux M, Ebrahim S, Hernandez Hernandez R, Jaff M, Kownator S, Naqvi T, Prati P, Rundek T, Sitzer M, Schminke U, Tardif JC, Taylor A, Vicaut E, Woo KS. Mannheim carotid intima-media thickness and plaque consensus (2004-2006-2011). An update on behalf of the advisory board of the 3rd, 4th and 5th watching the risk symposia, at the 13th, 15th and 20th European Stroke Conferences, Mannheim, Germany, 2004, Brussels, Belgium, 2006, and Hamburg, Germany, 2011. Cerebrovasc Dis. 2012;34(4):290–6.

67. Oudkerk M, Stillman AE, Halliburton SS, Kalender WA, Möhlenkamp S, McCollough CH, Vliegenthart R, Shaw LJ, Stanford W, Taylor AJ, van Ooijen PM, Wexler L, Raggi P. Coronary artery calcium screening: current status and recommendations from the European Society of Cardiac Radiology and North American Society for Cardiovascular Imaging. Int J Cardiovasc Imaging. 2008;24(6):645–71.

68. Russell K, Eriksen M, Aaberge L, Wilhelmsen N, Skulstad H, Gjesdal O, Edvardsen T, Smiseth OA. Assessment of wasted myocardial work: a novel method to quantify energy loss due to uncoordinated left ventricular contractions. Am J Physiol Heart Circ Physiol. 2013;305(7):H996–1003.

69. Manganaro R, Marchetta S, Dulgheru R, Ilardi F, Sugimoto T, Robinet S, Cimino S, Go YY, Bernard A, Kacharava G, Athanassopoulos GD, Barone D, Baroni M, Cardim N, Hagendorff A, Hristova K, López-Fernández T, de la Morena G, Popescu BA, Penicka M, Ozyigit T, Rodrigo Carbonero JD, van de Veire N, Von Bardeleben RS, Vinereanu D, Zamorano JL, Rosca M, Calin A, Moonen M, Magne J, Cosyns B, Galli E, Donal E, Carerj S, Zito C, Santoro C, Galderisi M, Badano LP, Lang RM, Oury C, Lancellotti P. Echocardiographic reference ranges for normal non-invasive myocardial work indices: results from the EACVI NORRE study. Eur Heart J Cardiovasc Imaging. 2019;20(5):582–90.

70. Bakija FZ, Tolvaj M, Szijártó Á, Tokodi M, Ferencz A, Lakatos BK, Ladányi Z, Kiss L, Szelid Z, Soós P, Merkely B, Bagyura Z, Kovács A, Fábián A. Long-term prognostic value of myocardial work analysis across obesity stages: insights from a community-based study. Int J Obes (Lond). 2025.

71. Spencer KT, Mor-Avi V, Gorcsan J, 3rd, DeMaria AN, Kimball TR, Monaghan MJ, Perez JE, Weinert L, Bednarz J, Edelman K, Kwan OL, Glascock B, Hancock J, Baumann C, Lang RM. Effects of aging on left atrial reservoir, conduit, and booster pump function: a multi-institution acoustic quantification study. Heart. 2001;85(3):272–7.

72. Tsang TS, Barnes ME, Gersh BJ, Takemoto Y, Rosales AG, Bailey KR, Seward JB. Prediction of risk for first age-related cardiovascular events in an elderly population: the incremental value of echocardiography. J Am Coll Cardiol. 2003;42(7):1199–205.

73. Morris DA, Belyavskiy E, Aravind-Kumar R, Kropf M, Frydas A, Braunauer K, Marquez E, Krisper M, Lindhorst R, Osmanoglou E, Boldt LH, Blaschke F, Haverkamp W, Tschöpe C, Edelmann F, Pieske B, Pieske-Kraigher E. Potential Usefulness and Clinical Relevance of Adding Left Atrial Strain to Left Atrial Volume Index in the Detection of Left Ventricular Diastolic Dysfunction. JACC Cardiovasc Imaging. 2018;11(10):1405–15.

74. Cameli M, Lisi M, Mondillo S, Padeletti M, Ballo P, Tsioulpas C, Bernazzali S, Maccherini M. Left atrial longitudinal strain by speckle tracking echocardiography correlates well with left ventricular filling pressures in patients with heart failure. Cardiovasc Ultrasound. 2010;8:14.

75. Wakami K, Ohte N, Asada K, Fukuta H, Goto T, Mukai S, Narita H, Kimura G. Correlation between left ventricular end-diastolic pressure and peak left atrial wall strain during left ventricular systole. J Am Soc Echocardiogr. 2009;22(7):847–51.

76. Modin D, Biering-Sørensen SR, Møgelvang R, Alhakak AS, Jensen JS, Biering-Sørensen T. Prognostic value of left atrial strain in predicting cardiovascular morbidity and mortality in the general population. Eur Heart J Cardiovasc Imaging. 2019;20(7):804–15.

77. Cameli M, Lisi M, Focardi M, Reccia R, Natali BM, Sparla S, Mondillo S. Left atrial deformation analysis by speckle tracking echocardiography for prediction of cardiovascular outcomes. Am J Cardiol. 2012;110(2):264–9.

78. Cereda A, Toselli M, Palmisano A, Vignale D, Khokhar A, Campo G, Bertini M, Loffi M, Andreini D, Pontone G, Patelli G, Sangiorgi GM, Tumminello G, Elia M, Iacovoni A, Carugo S, Rapezzi C, Colombo A, Giannini F, Esposito A. Coronary calcium score as a predictor of outcomes in the hypertensive Covid-19 population: results from the Italian (S) Core-Covid-19 Registry. Hypertens Res. 2022;45(2):333–43.

79. Badimon L, Bugiardini R, Cenko E, Cubedo J, Dorobantu M, Duncker DJ, Estruch R, Milicic D, Tousoulis D, Vasiljevic Z, Vilahur G, de Wit C, Koller A. Position paper of the European Society of Cardiology-working group of coronary pathophysiology and microcirculation: obesity and heart disease. Eur Heart J. 2017;38(25):1951–8.

80. Bray GA, Kim KK, Wilding JPH. Obesity: a chronic relapsing progressive disease process. A position statement of the World Obesity Federation. Obes Rev. 2017;18(7):715–23.

81. Heymsfield SB, Wadden TA. Mechanisms, Pathophysiology, and Management of Obesity. N Engl J Med. 2017;376(3):254–66.

82. Thorp AA, Schlaich MP. Relevance of Sympathetic Nervous System Activation in Obesity and Metabolic Syndrome. J Diabetes Res. 2015;2015:341583.

83. Chinali M, de Simone G, Roman MJ, Lee ET, Best LG, Howard BV, Devereux RB. Impact of obesity on cardiac geometry and function in a population of adolescents: the Strong Heart Study. J Am Coll Cardiol. 2006;47(11):2267–73.

84. Huang J, Li GA, Wang J, Jiao YW, Qian ZF, Fan L, Tang LM. Evaluation of subclinical left ventricular systolic dysfunction in obese patients by global myocardial work. Diabetol Metab Syndr. 2023;15(1):254.

85. Sahiti F, Morbach C, Cejka V, Tiffe T, Wagner M, Eichner FA, Gelbrich G, Heuschmann PU, Störk S. Impact of cardiovascular risk factors on myocardial work-insights from the STAAB cohort study. J Hum Hypertens. 2022;36(3):235–45.

86. Yang H, Huynh QL, Venn AJ, Dwyer T, Marwick TH. Associations of childhood and adult obesity with left ventricular structure and function. Int J Obes (Lond). 2017;41(4):560–8.

87. Olsen FJ, Skaarup KG, Lassen MCH, Johansen ND, Jensen GB, Schnohr P, Marott JL, Søgaard P, Gislason G, Svendsen JH, Møgelvang R, Aalen JM, Smiseth OA, Remme EW, Biering-Sørensen T. Association between myocardial work indices and cardiovascular events according to hypertension in the general population. Eur Heart J Cardiovasc Imaging. 2024;25(3):413–24.

88. Alenezi F, Ambrosy AP, Phelan M, Chiswell K, Abudaqa L, Alajmi H, Kisslo J, Velazquez EJ. Left Ventricular Global Longitudinal Strain Can Reliably Be Measured from a Single Apical Four-Chamber View in Patients with Heart Failure. J Am Soc Echocardiogr. 2019;32(2):317–8.

89. Salaun E, Casalta AC, Donal E, Bohbot Y, Galli E, Tribouilloy C, Hubert S, Magne J, Mancini J, Renard S, Avierinos JF, Maysou LA, Lavoute C, Szymanski C, Haentjens J, Habib G. Apical four-chamber longitudinal left ventricular strain in patients with aortic stenosis and preserved left ventricular ejection fraction: analysis related with flow/gradient pattern and association with outcome. Eur Heart J Cardiovasc Imaging. 2018;19(8):868–78.

9 Bibliography of the candidate

9.1 Bibliography related to present thesis

1. **Zhubi Bakija F**, Tolvaj M, Szijártó Á, Tokodi M, Ferencz A, Lakatos B, Ladányi Z, Kiss L, Szelid Z, Soós P, Merkely B, Bagyura Z, Kovács A, Fábián A. Long-Term Prognostic Value of Myocardial Work Analysis Across Obesity Stages: Insights from a Community-Based Study. International Journal of Obesity. 2025 Aug 6 doi: 10.1038/s41366-025-01863-w
   IF: **3.8**

2. **Zhubi Bakija F**, Bagyura Z, Fábián A, Ferencz A, Kiss L, Szenczi O, Vadas R, Dósa E, Nguyen DT, Csobay-Novák C, Jermendy ÁL, Szelid Z, Soós P, Kovács A, Merkely B. Long-term prognostic value of left atrial longitudinal strain in an elderly community-based cohort. Geroscience. 2023 Feb.doi: 10.1007/s11357-022-00673-
   IF: **5.3**

9.2 Bibliography not related to present thesis

1. Tolvaj M, **Zhubi Bakija F**, Fábián A, Ferencz A, Lakatos B, Ladányi Z, Szijártó Á, Edvi B, Kiss L, Szelid Z, Soós P, Merkely B, Bagyura Z, Tokodi M, Kovács A. Integrating Left Atrial Reservoir Strain Into the First-Line Assessment of Diastolic Function: Prognostic Implications in a Community-Based Cohort With Normal Left Ventricular Systolic Function. J Am Soc Echocardiogr. 2025 Mar 27. doi: 10.1016/j.echo.2025.03.012.
   IF: **6.0**
2. Tolvaj M, Tokodi M, Lakatos B, Fabian A, Ujvari A, **Zhubi Bakija F**, Ladanyi Z, Tarcza Z, Merkely B, Kovács A. Added predictive value of right ventricular ejection fraction compared with conventional echocardiographic measurements in patients who underwent diverse cardiovascular procedures December 2021.doi: 10.1556/1647.2021.00049
3. Bajraktari G, Rexhaj Z, Elezi S, **Zhubi-Bakija F**, Bajraktari A, Bytyçi I, Batalli A, Henein MY. Radial Access for Coronary Angiography Carries Fewer Complications

Compared with Femoral Access: A Meta-Analysis of Randomized Controlled Trials. J Clin Med. 2021 May 17. doi: 10.3390/jcm10102163.
IF: **4.964**

4. Bajraktari G, **Zhubi-Bakija F**, Ndrepepa G, Alfonso F, Elezi S, Rexhaj Z, Bytyçi I, Bajraktari A, Poniku A, Henein MY. Long-Term Outcomes of Patients with Unprotected Left Main Coronary Artery Disease Treated with Percutaneous Angioplasty versus Bypass Grafting: A Meta-Analysis of Randomized Controlled Trials. J Clin Med. 2020 Jul 14. doi: 10.3390/jcm9072231.
   IF: **4.242**
5. **Zhubi-Bakija F**, Bajraktari G, Bytyçi I, Mikhailidis DP, Henein MY, Latkovskis G, Rexhaj Z, Zhubi E, Banach M; International Lipid Expert Panel (ILEP). The impact of type of dietary protein, animal versus vegetable, in modifying cardiometabolic risk factors: A position paper from the International Lipid Expert Panel (ILEP). Clin Nutr. 2021 Jan. doi: 10.1016/j.clnu.2020.05.017.
   IF: **7.643**

10 Acknowledgements

First and foremost, I wish to express my deepest gratitude to my PhD supervisors, Dr. Attila Kovács and Dr. Alexandra Fábián, for their unwavering support, encouragement, and invaluable guidance throughout this four-year journey at Semmelweis University. Their commitment to scientific rigor and their thoughtful mentorship have been instrumental in shaping both my academic development and professional growth.

I am also sincerely grateful to Semmelweis University and to Professor Béla Merkely for fostering an inclusive academic environment and for providing opportunities for international students, such as myself, to pursue advanced studies at such a renowned institution. I feel truly privileged to have been part of this academic community.

My heartfelt thanks go to the echocardiography working group and the Budakalász team for their collaboration and support.

I am profoundly grateful to my husband and daughter, whose patience, understanding, and love sustained me through the most demanding times of my PhD studies.

I extend my gratitude to my parents and sisters for their lifelong sacrifices and limitless encouragement, which laid the foundation for everything I have achieved.

This accomplishment would not have been possible without the enduring support of all these individuals. To each of you, I am eternally grateful for your support in this challenging but greatly rewarding journey of my academic achievement.